AMPK activation by aldometanib alleviates inflammation and autoimmune disease via suppressing inflammatory T cell generation

Yu Zhou[1,7], Fengli Wang[1,2,7], Tao Wang[3,7], Yan He[4], Rongrong He[1], Mengsha Zhou[1], Xin Wang[1], Ke Zhang[1], Lihua Fan[1], Xinyue He[1], Cuiling Dong[1], Yazhen Hong[1], Chensong Zhang[1], Yuxuan Wang[1]*, Zhiqing Fan[1,5]*, Wen-Hsien Liu[1,5,6]*, Chenfeng Liu[2,8]*

[1] State Key Laboratory of Cellular Stress Biology, School of Life Sciences, Faculty of Medicine and Life Sciences, Xiamen University, Xiamen, 361102, China.

[2] School of Life Sciences, Anhui Medical University, Hefei, 230032, China.

[3] The Key Laboratory of Urinary Tract Tumors and Calculi, Department of Urology, The First Affiliated Hospital of Xiamen University, School of Medicine, Xiamen University, Xiamen, 361003,China.

[4] Department of Rheumatology and Clinical Immunology, the First Affiliated Hospital of Xiamen University, School of Medicine, Xiamen University, Xiamen, 361000, China.

[5] Zhongke Cell (Xiamen) Precision Medicine Technology Co., Ltd. Xiamen, 361000, China.

[6] State Key Laboratory of Vaccines for Infectious Diseases, Xiang An Biomedicine Laboratory, Xiamen University, Xiamen, 361102, China.

[7] These authors contributed equally

[8] Lead contact

*Correspondence: dwyxxking19@163.com (Y.W.), ZhongkeCell@163.com (Z.F.), whliu@xmu.edu.cn (W-H.L.), chenfengliu0607@ahmu.edu.cn (C.L.)

Abstract

Background: Aberrant T-cell activation and differentiation are central drivers of chronic inflammatory and autoimmune diseases. However, current therapies targeting T-cell function to ameliorate these pathological conditions frequently carry risks of immunotoxicity. AMPK activators have been shown to exert therapeutic effects in metabolic disorders and preventive effects against tumour progression; however, it is not clear whether they can modulate T-cell responses to suppress inflammatory and autoimmune pathologies.

Methods: We utilized an *in vitro* OVA-triggered OT-II $CD4^+$ T cell model to examine the functional changes in T cells induced by diverse AMPK agonists. Aldometanib, a selective lysosomal AMPK activator that mimics glucose starvation, was further characterized for its effects on T-cell function. Mechanistic studies were performed via RNA-sequencing, immunoblotting, and rescue experiments using a CRISPR-Cas9 system and mixed bone marrow chimeras. The therapeutic efficacy of aldometanib was assessed in murine models of acute lung injury, allergic inflammation and chronic colitis, as well as in spontaneous lupus-prone mice. We further investigated whether aldometanib suppresses cytokine production in peripheral blood mononuclear cells (PBMCs) isolated from patients with systemic lupus erythematosus (SLE) under *ex vivo* conditions, providing preliminary proof-of-concept evidence. Finally, we compared the effects on immune homeostasis, safety profile, and tissue toxicity of aldometanib, rapamycin, and MK2206.

Results: We analyzed the effects of AMPK activators on T cells and reported that aldometanib significantly inhibited IFN-γ secretion by $CD4^+$ T cells while preserving cell survival. Aldometanib suppressed T-cell activation, proliferation, and differentiation via AMPK activation and PTEN-associated programs. Moreover, compared with that of rapamycin, aldometanib had a more favourable preliminary safety profile in terms of thymocyte development and immune homeostasis. Additionally, aldometanib alleviated tissue inflammation and reduced inflammatory T-cell generation in lung injury and chronic colon inflammation. Furthermore, aldometanib ameliorated lymphadenopathy, lupus nephritis, and aberrant

inflammatory T-cell generation and autoantibody production in lupus-prone mice. Notably, proinflammatory cytokine production by T cells was markedly reduced in PBMCs from patients with SLE *ex vivo*.

Conclusion: The findings of this study demonstrate that aldometanib alleviates inflammatory disorders by suppressing T-cell activation and the generation of inflammatory T cells via AMPK-dependent and PTEN-associated programs, providing preliminary proof-of-concept evidence for further investigation of aldometanib as a potential therapeutic strategy for inflammatory and autoimmune diseases.

Keywords: Aldometanib; AMPK; T cell differentiation; Inflammation; Autoimmune disease; Systemic lupus erythematosus

Highlights

- Aldometanib inhibits T cell activation and cytokine production via AMPK activation.
- Aldometanib regulates a PTEN-associated program to attenuate T cell response.
- Aldometanib ameliorates acute and allergic lung injury and gut inflammation.
- Aldometanib alleviates murine lupus and curbs proinflammatory cytokine production by T cells in SLE patients.

Introduction

Dysregulated helper T (Th) cell differentiation drives the progression of multiple autoimmune and inflammatory diseases, including SLE, multiple sclerosis (MS), colitis, and lung inflammation, which are characterized by the excessive production of proinflammatory cytokines including IFN-γ, IL-4 and IL-17A[1, 2]. Although JAK inhibitors and anti-cytokine therapeutics have been widely used for the treatment of SLE, psoriasis, MS and colitis[3, 4], these therapies exhibit limited efficacy in only a subset of patients and cause substantial adverse effects because of disease heterogeneity derived from genetic, environmental, and epigenetic factors. Such side effects include immune-mediated enteritis, high fever, recurrent infections, and hepatorenal toxicity [5, 6]. Therefore, the precise modulation of pathogenic T-cell differentiation represents a critical unmet medical need for developing safer and more effective therapies against inflammatory and autoimmune diseases.

The mTOR/AKT/FoxO1 axis critically orchestrates T-cell differentiation and functions primarily by regulating cellular metabolism, indicating that targeting this axis is a key intervention strategy for treating T-cell-mediated inflammatory diseases[7-9]. Specifically, mTORC1 drives glycolysis via HIF-1α to promote Th1/Th17 differentiation[10], whereas mTORC2 activates AKT to phosphorylate and inhibit FoxO1, thus repressing the expression of Treg-related functional markers, including CTLA-4 and CD25[11]. Recent studies have demonstrated that inhibiting downstream mTOR effectors, such as HIF-1α, and restricting glycolytic metabolism can suppress inflammatory T-cell differentiation and ameliorate inflammatory pathologies[12, 13]. Pharmacological inhibition of AKT using agents such as LY294002 and fingolimod suppresses effector T-cell differentiation through the PI3K-PTEN or AKT/mTOR cascades, and such intervention strategies are clinically utilized to treat psoriasis and multiple sclerosis[14, 15]. In clinical settings, sirolimus, an mTORC1 inhibitor, has become a targeted therapy for specific autoimmune diseases such as autoimmune lymphoproliferative syndrome (ALPS), achieving a complete response in more than 90% of paediatric patients[16]. It also shows promising therapeutic potential in other disorders, including SLE (NCT00779194)

and systemic sclerosis, by reducing steroid dependence and improving clinical outcomes[17]. Its derivative, everolimus, can also synergize with PD-L1 blockade to enhance antitumour immunity[18]. Despite the well-documented lifespan-extending effects of rapamycin, both AKT inhibitors and rapamycin impair physiological growth and organ function and compromise immune cell survival and effector activity, highlighting their dual roles in immune regulation[19, 20]. Thus, precisely rewiring T-cell metabolism to maintain immune homeostasis while preserving T-cell viability is critical for developing safer next-generation inflammatory and autoimmune disease therapies.

AMP-activated protein kinase (AMPK) maintains cellular homeostasis by sensing the intracellular energy status through the ratios of AMP/ATP and ADP/ATP and is principally regulated by the kinases LKB1 and CaMKKβ. AMPK can be activated in lysosomes, the cytoplasm, and mitochondria via distinct mechanisms, enabling precise spatiotemporal control of metabolic homeostasis[21, 22]. Lysosomal AMPK activation relies on PEN2-mediated recruitment of the γ-secretase complex and LKB1, which phosphorylates AMPKα at Thr172 in an ATP depletion-independent manner [23]. Activated AMPK phosphorylates ACC1 and HMGCR to suppress fatty acid synthesis, upregulates UCP1, and inhibits mTORC1 signaling, thus coupling cellular energy status with cell growth and proliferation[21, 22]. Thus, tightly controlled AMPK activity is crucial for cellular homeostasis and function.

Multiple AMPK activators are currently available or are under preclinical and clinical investigation. As a frontline therapeutic drug against type 2 diabetes, metformin indirectly increases AMPK activity: it blocks mitochondrial complex I to increase the AMP/ATP ratio[24]. Although metformin exhibits potent immunomodulatory effects *in vivo*, its biological actions predominantly target the liver and intestine [25-27]. MK-8722, a pan-AMPK agonist, improved glucose homeostasis; however, it induced cardiac hypertrophy as an adverse effect[28]. As a cell-permeable analogue of adenosine, 5-aminoimidazole-4-carboxamide ribonucleoside (AICAR) undergoes phosphorylation mediated by adenosine kinase to produce ZMP; this metabolite simulates AMP and thus induces AMPK signaling

activation[29]. Despite extensive research efforts, direct pharmacological AMPK agonists still face substantial limitations, including off-target effects, low bioavailability, and dose-dependent gastrointestinal toxicity[30]. These drawbacks likely result from poor compartmental specificity, as conventional agonists induce unphysiological, widespread AMPK activation across all subcellular compartments.

Aldometanib is a novel AMPK activator that selectively triggers the lysosomal AMPK pathway by blocking the binding of aldolase to fructose-1,6-bisphosphate (FBP), thus mimicking cellular starvation or caloric restriction. It suppresses aldolase activity to induce AMPKα Thr172 phosphorylation, driving downstream metabolic reprogramming, including the inhibition of ACC1 phosphorylation, the enhancement of mitochondrial biogenesis through PGC-1α upregulation, and the promotion of autophagy. Consistently, aldometanib confers robust metabolic benefits: it reduces blood glucose levels, ameliorates hepatic steatosis in obese mice, and prolongs lifespan through AMPK activation in the muscle and liver. Compared with other AMPK agonists, aldometanib activates AMPK across diverse tissues and cell types[31].

In this study, we report that aldometanib markedly suppresses proinflammatory cytokine production during T-cell activation, proliferation, and Th-cell differentiation and mitigates lung injury and chronic inflammation. Strikingly, aldometanib alleviated lymphadenopathy and lupus nephritis in a mouse model of SLE and inhibited inflammatory T-cell generation in patients with SLE. These findings support further investigations of the use of aldometanib as a potential therapeutic strategy for treating inflammatory and autoimmune diseases.

Materials and methods

Patient sample collection and processing

Human peripheral blood samples were harvested from active SLE patients at the Department of Rheumatology, the First Affiliated Hospital of Xiamen University. This clinical research scheme received ethical approval from Xiamen University (Approval No. XMYY-2024KY218). All patients were confirmed to be in the active

phase of SLE based on positive anti-nuclear antibody (ANA) and elevated immunoglobulin levels. Written informed consent was acquired from every enrolled participant before sample collection. Detailed clinical characteristics of all patients are outlined in **Table S1**.

Mouse models

C57BL/6J (JAX 000664), *Rag1*$^{-/-}$ (JAX 003145), OT-II (JAX 004194), and MRL-Faslpr/J (JAX 000482), *Pten*$^{fl/fl}$ (JAX 006440), Cas9 (JAX 026175) mice were purchased from Jackson laboratory. *Prkaa1*$^{fl/fl}$ (JAX 014141) and *Prkaa2*$^{fl/fl}$ mice (JAX 014142) were kindly provided by Dr. Chensong Zhang (Xiamen University). AMPK knockout (KO) mice, generated by crossing AMPKα1/2$^{fl/fl}$ (*Prkaa1*$^{fl/fl}$; *Prkaa2*$^{fl/fl}$) mice with VAV1 Cre mice (JAX 035670) were provided by Dr. Jianfeng Wu (Xiamen University). For the experiments in investigating the effects of aldometanib, rapamycin, MK-2206 on immune homeostasis and development, 4 week-old mice were used, whereas other experiments utilized 6-8-week-old adult mice. All animal manipulations complied with the Laboratory Animal Care and Use Guidelines issued by Xiamen University, and all *in vivo* protocols were authorized by the Xiamen University Animal Research Ethics Committee (Approval ID: XMULAC20230600).

To investigate whether aldometanib affects thymocyte development and immune homeostasis, 4-5 week-old mice received daily intragastric (i.g.) administration of aldometanib (2 mg/kg), rapamycin (1.5mg/kg), MK-2206 (4mg/kg) for 24 days. Immune organs (spleen, thymus, LNs and bone marrows) were subsequently collected for pathological and flow cytometry analysis. For the experiments in investigating the effects of aldometanib on autoimmune disease progression, 3-month-old MRL-Fas^{lpr}/J mice were treated with daily i.g. administration of aldometanib (2 mg/kg) for 3 months, followed by collection of immune organs and kidney tissues for histological and flow cytometric analysis.

OVA-stimulated OT-II CD4$^+$ T cell system

This system and relevant cell culture conditions were consistent with our previous

work[32]. Briefly, $CD11c^+$ DCs were isolated from *Rag1*$^{-/-}$ mouse splenocytes and pulsed with OVA (200 μg/mL, Sigma, Missouri, USA) for 24 h (day -1 to 0). Next, naïve OT-II $CD4^+$ T cells were co-cultured with OVA-pulsed DCs. Aldometanib (2 nM) was added at the indicated time points. On day 3.5, cells were stimulated with ionomycin (Yeasen, Shanghai, China) and PMA (Sigma, Missouri, USA), cytokines were blocked by GolgiPlug from BD (New Jersey, USA) for 4 h, followed by standard intracellular cytokine staining. Using OVA-OT-II system, we evaluated the effects of aldometanib and pharmacological interventions including rapamycin, MK2206, AICAR, MK8722, metformin, recilisib, MHY1485, VO-Ohpic, Bay3827 and compound C on T-cell function, all the compounds were obtained from Med Chem Express (Monmouth Junction, USA).

T cell polarization

Naïve $CD4^+$ T cells were purified with a Miltenyi isolation kit (Bergisch Gladbach, Germany) and cultured under TCR stimulation using anti-CD3/CD28 antibodies at 3 μg/mL. IL-2 (20 ng/mL) and IL-12 (10 ng/mL) were supplemented to drive Th1 differentiation, whereas IL-6 (50 ng/mL) and TGF-β (1 ng/mL) were added to induce Th17 polarization. TGF-β (2 ng/mL) combined with IL-2 (10 ng/mL) were required for iTreg generation. All antibodies and cytokines were obtained from BioLegend (San Diego, CA, USA).

T cell proliferation assay

CFSE staining kits (Thermo, Massachusetts, USA) were utilized to detect T cell proliferation. In short, isolated naïve OT-II $CD4^+$ T lymphocytes were labeled with 0.5 μM CFSE in prewarmed PBS for 20 min at 37 °C, and the labeling reaction was terminated with complete RPMI 1640 medium. After 3.5 days of stimulation with OVA, flow cytometry was applied to measure CFSE dilution and assess T cell proliferative capacity.

RNA-seq analysis

For transcriptomic analysis, OT-II $CD4^+$ T cells were sorted at 2.5 days after OVA

stimulation. Total RNA was extracted with the RNeasy Kit (Qiagen, Hilden, Germany). One microgram of RNA from each sample was used for transcriptome sequencing on the BGISEQ-500 platform (BGI, Wuhan, China). Differentially expressed genes (DEGs) were filtered, and GSEA was performed to enrich biological functions and signaling pathways with support from the Mouse Genome Informatics (MGI) database (http://www.informatics.jax.org). All raw RNA-seq reads were uploaded to the NCBI SRA database under BioProject accession PRJNA1370081.

OT-II transfer model of acute lung injury

An OT-II $CD4^+$ T cell-mediated lung injury mouse model was generated as previously described[33]. In brief, *Rag1*$^{-/-}$ mice received intravenous injection of 2×10^6 naïve OT-II $CD4^+$ T cells on day 0. On day 1, each mouse was intraperitoneally immunized with an OVA/Alum mixture (100 μg OVA and 100 μL alum, Sigma, Missouri, USA). Animals in the aldometanib group were given daily intragastric (i.g.) dosing of aldometanib at 2 mg/kg from day 1 to 8. From day 8 to 11, all mice underwent daily 30-minute aerosol inhalation of 2% (w/v) OVA diluted in PBS. All animals were euthanized on day 12 for histological assessment and flow cytometric detection.

OVA-induced asthma model

To construct the OVA-induced asthma model, mice were sensitized by intraperitoneal injection of OVA/Alum (100 μg OVA plus 100 μL Alum) on day 0, 7, and 14. Mice in the Aldometanib group received intragastric (i.g.) treatment with Aldometanib (2 mg/kg) from day 2 to 17. From day 18 to 21, all mice underwent daily 30-minute aerosol inhalation of 2% (w/v) OVA diluted in PBS. All animals were euthanized on day 22 for histological assessment and flow cytometric detection.

Bone marrow reconstitution

Mixed bone marrow chimeric mice (BMC) were generated by reconstituting lethally irradiated *Rag1*$^{-/-}$ mice (7 Gray) with mixed bone marrow cells at a 20:80 ratio[34].

The bone marrow cell mixtures were isolated from either WT or *Prkaa1/2*$^{fl/fl}$;Vav-Cre mice (KO) and T cell-deficient (*Tcrb*$^{-/-}$ and *Tcrbd*$^{-/-}$, TCD) mice. This 20:80 reconstitution ratio ensures that the regenerated T cells are exclusively derived from *Prkaa*1/2-deficient (KO) or WT donor bone marrow cells, while eighty percent of the TCD bone marrows sustained near-physiological non-T-cell haematopoietic development, compensating for potential functional defects in non-T-cell populations from 20% of the KO cells. Each recipient mouse was adoptively transferred with 5 × 10^6 mixed bone marrow cells after T cell depletion via tail vein injection. BMCs were verified by flow cytometry after eight weeks reconstitution. These validated chimeric mice were used to evaluate the protective effects of aldometanib on allergic airway inflammation.

T cell induced colitis

Rag1$^{-/-}$ mice were intraperitoneally transferred with 4 × 10^5 naïve CD4$^+$ T cells from WT or *Ampk*α1/2$^{-/-}$ mice on day 0 to establish a colitis model. The aldometanib-treated mice received daily i.g. administration of aldometanib (2 mg/kg) until day 45. After 7 weeks of treatment, colon tissues and mesenteric lymph nodes were harvested for evaluation.

Prkaa1* and *Pten* deletion *in vitro

For *Prkaa1* deletion in OT-II Cas9 CD4$^+$ T cells, we designed specific small guide RNAs (sgRNAs) targeting mouse *Prkaa1*(**Table S2**). CD4$^+$ T cells were purified and activated using OVA-OT-II system. For CRISPR-Cas9-mediated *Prkaa1* editing, retroviruses carrying *Prkaa1*-targeting sgRNA were generated and used to infect activated CD4$^+$ T cells. Polybrene (Sigma-Aldrich, Missouri, USA) and IL-2 (BioLegend, San Diego, USA) were supplemented during viral transduction to improve infection efficiency and cell survival. For *Pten* deletion, purified *Pten*$^{fl/fl}$ CD4$^+$ T cells were stimulated with TCR stimulation under Th1 differentiation conditions. Cre-recombinase encoding retroviruses were produced and transduced into these activated T cells to deplete endogenous PTEN. Cells were then treated with

aldometanib for subsequent functional assays.

Isolation of immune cells from mouse tissues.

Briefly, harvested tissues (lung, colon and kidney) were mechanically dissociated and digested in complete RPMI-1640 medium supplemented with collagenase Type IV (1 mg/mL, Worthington Biochemical, New Jersey, USA) and DNase I (0.1 mg/mL, Sangon Biotech, Shanghai, China) at 37 °C for 60 min. Digested tissue suspensions were gently homogenized, filtered and centrifuged. Cell pellets were resuspended and subjected to density gradient centrifugation with Percoll (Cytiva, Massachusetts, USA) to enrich leukocytes. Finally, purified immune cells were resuspended in FACS buffer for subsequent staining and flow cytometric analysis.

AMPK Activation in Lymph Nodes Induced by Aldometanib

C57BL/6 mice were orally administered with vehicle control, 2 or 4 mg/kg aldometanib. Two hours after drug administration, mouse lymph nodes were collected, snap-frozen instantly, and then homogenized in lysis buffer, the lysis buffer has been described previously[32]. Tissue homogenates were centrifuged to collect supernatants for subsequent immunoblot analysis.

Immunoblot assay

Denatured protein samples were resolved on 10% SDS-PAGE gels with a constant voltage of 80 V for 30 min in the stacking gel and 120 V for 1 h in the separating gel. Separated proteins were electrophoretically transferred onto PVDF membranes (Merck, Darmstadt, Germany) at a constant current of 0.25 A for 2.5 h. After transfer, PVDF membranes were washed, blocked with 5% (w/v) non-fat milk, and subsequently incubated with primary antibodies against target proteins overnight at 4 °C. Primary antibodies included AMPKα (#5831), Phospho-AMPKα (Thr172) (#2535), Phospho-Akt (Thr308) (#2965), Phospho-Akt (Ser473)(#4060), pan-Akt (#4685), PTEN (#9188), S6 Ribosomal Protein (#2217), Phospho-S6 Ribosomal Protein (Ser235/236) (#4857), and β-Actin (#4970) (all from CST, Massachusetts,

USA). After primary antibody incubation, membranes were washed and incubated with HRP-conjugated species-matched secondary antibodies (CST) for 1 h at room temperature. ECL chemiluminescence substrate (Thermo, Massachusetts, USA) was applied to visualize protein bands, which were then captured with the Amersham Imager 600 detection system (Cytiva, Massachusetts, USA).

Hematoxylin-eosin staining

Fixed and embedded tissue specimens were sliced into serial 5 μm-thick sections. After high-temperature dewaxing, hematoxylin-eosin staining was automatically performed using the HistoCore SPECTRA ST automated slide stainer (Leica Biosystems Nussloch GmbH, Nussloch, Germany).

Immunofluorescence

Mouse kidney were fixed and permeabilized with BD fixation/permeabilization solution (New Jersey, USA) for 24 h, and then embedded in OCT. Serial frozen sections were sliced using a Leica cryostat. Kidney sections were incubated with rabbit anti-C3 antibody (Selleck, Texas, USA), followed by incubation with a goat anti-rabbit secondary antibody (AF555, Thermo, Massachusetts, USA) to detect renal C3 deposition. An anti-mouse IgG antibody was used to display glomerular IgG deposition. All stained sections were imaged using a fluorescence microscope to observe the distribution of IgG and C3 in renal glomeruli.

ELISA

Blood and urine samples were collected from mice for antibodies, complement and albumin detection. Serum was separated from blood samples via centrifugation at 4000g for 20 minutes. The serum levels of anti-dsDNA (Alpha Diagnostic International, Texas, USA), ANA (Zcibio, Shanghai, China), and Complement 3 (C3) (Neobioscience, Shenzhen, China), as well as urinary albumin levels (Zcibio), were measured. In brief, diluted serum or urine samples were incubated in ELISA plates, and subsequently incubated with HRP-conjugated antibodies. After washing, TMB

substrate solution was added for chromogenic reaction, and the reaction was finally terminated by stop buffer. A microplate spectrophotometer was applied to measure absorbance at 450 nm (Thermo Fisher Scientific, Massachusetts, USA).

Serum and urine biochemical analysis

The obtained serum and fresh urine samples were subjected to routine biochemical detection using a fully automatic veterinary biochemical analyzer (BS-240 Vet, Mindray, Shenzhen, China) according to the standard operating procedures. LDH, UA and Urea of serum or urine were quantitatively analyzed to evaluate the renal functional changes in mice.

Flow cytometry and intracellular cytokine staining

For cell surface marker detection, we stained samples on ice for 15 min using indicated panels of fluorophore-conjugated antibodies against CD4, CD8, TCRβ, CD44, CD25, CD62L, CD69, CD71, ICOS, CD11b, Gr1, F4/80, Siglec-F (CD170), MHC-II, CD45, CD11c, alongside Fixable Viability Dye. Intracellular proteins (Foxp3, CTLA4, Eomes, T-bet, Blimp-1) and cytokines (IL-17A, IFN-γ, TNF-α, IL-4) were labeled with matching antibodies. After surface staining, cells were fixed and permeabilized with eBioscience reagents (Massachusetts, USA) on ice for 30 min, followed by 1 h of intracellular staining in the dark. To measure cytokine production, cells were pre-stimulated with PMA plus ionomycin and treated with GolgiPlug for 4 h before surface staining. Flow cytometry data were acquired on a BD LSR Fortessa cytometer and analyzed with FlowJo v10 software. All antibodies were obtained from Thermo Fisher, BioLegend or BD Biosciences.

Isolation and stimulation of PBMCs

PBMCs were isolated from patients with SLE and healthy volunteers, using Ficoll-Paque™ Plus density-gradient medium (Cytiva, Massachusetts, USA). Briefly, fresh blood diluted in PBS was layered onto Ficoll-Paque medium, centrifuged without brake acceleration, and the PBMC-rich interphase was harvested, washed

twice in PBS, and reconstituted in complete RPMI-1640 medium. Purified PBMCs were plated at 4×10^5 cells per well and cultured with anti-human CD3/CD28 antibodies alongside aldometanib for 48 h, then restimulated for 4 h using an activation mixture of PMA, ionomycin and GolgiPlug. Cells were then harvested for surface and intracellular staining. Human-specific antibodies were purchased from BD Biosciences.

Statistical analysis

All statistical analyses were performed using GraphPad Prism 8.0. For two-group comparisons, the unpaired Student's t test was applied for independent samples, whereas the paired Student's t test was used when clinical samples with or without aldometanib treatment were compared. For analyses involving more than two groups, one-way ANOVA followed by Tukey's post-hoc test was used for multiple-group comparisons. Before parametric tests (t test and one-way ANOVA) were performed, the Shapiro-Wilk test was used to assess data normality. For data that did not meet the normality assumption, the nonparametric Mann-Whitney U test or Kruskal-Wallis test was adopted for statistical analysis. All assumptions for parametric tests were fully evaluated prior to analysis. Survival data were analyzed using the Kaplan–Meier method, with intergroup differences evaluated by the log-rank test. Sample sizes were determined on the basis of published literature and our preliminary experimental data to ensure sufficient statistical power while reducing animal usage. For experiments with small sample sizes (n=3-4), we acknowledge that conventional normality testing has limited statistical power; therefore, we also considered corresponding nonparametric alternatives where appropriate. It should be emphasized that for datasets with small sample sizes, we generally performed at least two independent replicate experiments to ensure the accuracy and reproducibility of our results. Data are presented as the means ± standard deviations (SDs). Differences with $p < 0.05$, $p < 0.01$, $p < 0.001$, or $p < 0.0001$ were considered statistically significant; ns denotes no significant difference. All figure summaries and layouts were generated using Adobe Illustrator (V27.0).

Results

Aldometanib Activates AMPK in T Cells to Inhibit Proinflammatory Cytokine Production.

To evaluate the effects of AMPK activators, such as metformin, AICAR, MK8722, and aldometanib on T-cell function, we employed an *in vitro* OVA/dendritic cell (DC)-stimulated OT-II cell activation model (OVA-OT-II system) (**Fig. 1A**). The results revealed that the classic AMPK activators metformin, AICAR, and MK8722 had little suppressive effect on T-cell function, as assessed by IFN-γ production by OT-II T cells, except for 1 μM MK8722, and did not affect T-cell survival (**Fig. 1B, C**). In contrast to these classic AMPK activators, aldometanib induced TCR/CD28-stimulated AMPK activation and dramatically inhibited IFN-γ production (**Fig. 1D-F**). Importantly, the effective concentration (0.5-5 nM) of aldometanib had a minimal effect on T-cell survival (**Fig. 1G**). These results demonstrate that compared with other AMPK activators, aldometanib suppresses $CD4^+$ T-cell cytokine secretion more potently and requires lower working concentrations while maintaining cell viability.

To determine whether aldometanib attenuated Th cell function, we subsequently performed an *in vitro* Th cell polarization assay. The results showed that aldometanib markedly inhibited IFN-γ and IL-17A secretion (**Fig. 1H–J**). Interestingly, the differentiation of $Foxp3^+$ Tregs clearly increased in response to aldometanib treatment (**Fig. S1**), indicating that aldometanib controls inflammatory T-cell function and promotes the introduction of Tregs. To test whether the inhibition of T-cell function by aldometanib depends on AMPK activation, we designed *Prkaa1* small guide RNAs (sgRNAs) and utilized CRISPR-Cas9-mediated gene deletion in $CD4^+$ T cells from OT-II Cas9 mice (**Fig. 1K**). Aldometanib obviously inhibited IFN-γ secretion in non-targeting control (NTC) sgRNA-transduced OT-II cells; however, AMPK deletion (*Prkaa1* sgRNA) in OT-II cells fully restored the reduction in cytokine production induced by aldometanib (**Fig. 1L**). Furthermore, Th1 polarization was induced in *Ampkα*1/2-knockout (KO) $CD4^+$ T cells with or without the use of aldometanib. Our data revealed that Th1 polarization was not affected by *Ampkα*1/2

deletion and that the inhibitory effect of aldometanib on Th1 polarization was completely abolished in *Ampkα*1/2-KO $CD4^+$ T cells (**Fig. 1M**), suggesting that aldometanib regulates T-cell function through an AMPK-dependent pathway. Together, these results demonstrate that aldometanib suppresses proinflammatory cytokine production by $CD4^+$ T cells via AMPK activation.

Aldometanib Inhibits T-Cell Activation and Proliferation.

T-cell activation and proliferation support T-cell function, a process marked by the early upregulation of CD69, CD25, CD44 and differentiation-associated molecules, including ICOS and CD71. We evaluated the effects of aldometanib on the expression of these markers during T-cell activation. Through co-staining for the naive T-cell marker CD62L and activation markers, we identified two cell populations designated P1 (early activation) and P2 (normal activation). Aldometanib treatment downregulated CD69 and CD25 expression and restrained initial T-cell activation. This compound also reduced the frequency and expression of CD44 (**Fig. S2A–C**). Furthermore, the mean fluorescence intensities (MFIs) of ICOS and CD71 were reduced in the presence of aldometanib, demonstrating that aldometanib impaired T-cell activation and early differentiation (**Fig. S2D**). Moreover, we employed a CFSE dilution assay to monitor T-cell proliferation and observed that aldometanib significantly suppressed T-cell division, especially in later generations (P5–P8) (**Fig. S3A-B**). Analysis of cytokine production across proliferative generations (P2–P8) revealed that aldometanib markedly inhibited cytokine secretion, most prominently within the P2 population (**Fig. S3C–H**). Collectively, these data demonstrate that aldometanib suppresses T-cell activation and proliferation.

Since dendritic cell (DC) function is essential for initiating T-cell activation, we investigated whether aldometanib modulates DC antigen presentation during T-cell priming. To define the window through which T-cell activation is susceptible to aldometanib, we treated cells with aldometanib either before T-cell priming (Days -1~0) or at multiple time points following T-cell activation (Days 0~4) using the OVA-OT-II system (**Fig. S4A**). The results indicated that treatment with aldometanib

significantly suppressed IFN-γ production by OT-II cells after T-cell priming (Days 1~4) and slightly affected antigen presentation by DCs (Days -1~0) (**Fig S4B**). Collectively, our results demonstrate that aldometanib restrains cytokine production by T cells mainly by affecting T-cell activation and proliferation and also modulating antigen presentation by DCs.

Aldometanib Regulates T-cell Function via a PTEN-associated Program.

To explore the molecular mechanism through which aldometanib regulates T-cell activation and differentiation, we performed transcriptomic profiling of OT-II $CD4^+$ T cells following OVA stimulation. PCA revealed distinct transcriptomic signatures in the aldometanib-treated T cells compared with those in naive and activated controls, indicating robust transcriptional reprogramming (**Fig. 2A**). A KEGG enrichment analysis revealed that aldometanib downregulated oxidative phosphorylation, glucose metabolism, and glycolysis pathways (**Fig. 2B**), consistent with the canonical metabolic regulatory function of AMPK. An additional pathway analysis confirmed that the transcription of PI3K-AKT/mTOR signaling-related genes was repressed after treatment with aldometanib (**Fig. 2C**). Immunoblotting analyses further confirmed that aldometanib reduced the phosphorylation of AKT and S6, which are key indicators of mTORC1 activation (**Fig. 2D**). Given the essential function of AKT/mTOR signaling in T-cell lymphocytes, we examined the expression of functional regulators and observed that the expression levels of CTLA-4, Eomes, T-bet, and Blimp1 decreased after treatment with aldometanib (**Fig. 2E–F**).

Rescue experiments using the AKT activator recilisib and the mTOR activator MHY1485 revealed that both of these activators partially restored the impairment of cytokine production induced by aldometanib (**Fig. S5A**). Moreover, pharmacological inhibition of AKT/mTOR signaling via rapamycin or MK2206 suppressed IFN-γ secretion but caused severe T-cell cytotoxicity (**Fig. S6**). These findings indicate that aldometanib inhibits T-cell function through mechanisms beyond simple AKT/mTOR suppression.

In addition to AKT/mTOR signaling, the transcriptomic analysis revealed that

aldometanib also suppressed the NF-κB signaling pathway and upregulated *Pten* and *Foxo1* transcription (**Fig. 2G**). PTEN, a well-known phosphatase, maintains cell homeostasis, differentiation and function. Pharmacological inhibition of PTEN with VO-Ohpic fully rescued the aldometanib-mediated defects in T-cell function in both the OVA-OT-II model and *in vitro* Th1 differentiation cultures (**Fig. 2H–I**). PTEN inhibition also attenuated the aldometanib-induced suppression of CTLA-4, Eomes, and T-bet (**Fig. 2J**). To exclude off-target effects of chemical inhibition, we generated *Pten*-deficient $CD4^+$ T cells by transducing $Pten^{fl/fl}$ $CD4^+$ T cells with Cre-expressing retroviruses. *Pten* deficiency nearly completely abrogated the inhibitory effects of aldometanib on IFN-γ, T-bet and CTLA-4 expression in Th1 cells (**Fig. S5B, Fig. 2K–L**). Collectively, these results demonstrate that aldometanib modulates T-cell function primarily through a PTEN-associated program.

To further confirm whether the aldometanib-mediated regulation of T-cell activation relies on AMPK and PTEN-associated program, we stimulated WT and *Ampkα*1/2-KO $CD4^+$ T cells via TCR/CD28 signaling. The results showed that aldometanib reduced the phosphorylation of S6 in WT $CD4^+$ T cells; however, these effects were completely abrogated in *Ampkα*1/2-KO $CD4^+$ T cells (**Fig. S7A)**. Moreover, aldometanib failed to downregulate the surface expression of the T-cell activation markers CD69, CD44 and ICOS on AMPK-deficient T cells as well as CTLA-4 and T-bet expression under Th1 polarization(**Fig. S7B-C)**. These results indicate that AMPK is required for aldometanib-mediated suppression of T-cell activation. We next assessed the contribution of PTEN-associated program to the regulation of T-cell activation by aldometanib. Consistent with our results of cytokine assays, treatment with recilisib or MHY1485 only slightly restored the inhibition of T-cell activation by aldometanib. In contrast, the PTEN inhibitor VO-Ohpic fully reversed the aldometanib-mediated suppression of T-cell activation(**Fig. S7D-E)**. Collectively, these data demonstrate that aldometanib regulates $CD4^+$ T-cell activation and function through AMPK activation and PTEN-associated program.

Aldometanib Exerts a Favourable Preliminary Safety Profile Regarding

Peripheral Immune Homeostasis and T-cell Development

Despite the clinical potential of rapamycin and MK2206 in transplant rejection and autoimmune disease treatment, their toxic effects on immune development and homeostasis limit their application. We further investigated the *in vivo* effects of aldometanib on immune organs and immune homeostasis. Oral aldometanib administration rapidly activated AMPK in mouse lymph nodes within 2 hours, confirming its effect on immune tissues (**Fig. 3A**). We then treated the mice with aldometanib, rapamycin, or MK2206 for 24 days at previously validated doses[35, 36]. All three treatments caused mild body weight loss (**Fig. 3B**), whereas MK2206 induced severe weight loss and approximately 30% mortality (**Fig. 3B-C**). Rapamycin and MK2206 significantly reduced the size and cellularity of the thymus, spleen, peripheral LNs, and mLNs, whereas aldometanib did not obviously alter these immune organs (**Fig. 3D-E**).

Consistent with organ-level changes, rapamycin and MK2206 markedly decreased thymic DP and CD4/CD8 SP cell populations. Aldometanib did not disturb thymic T-cell development, with only a slight reduction observed in the number of CD4 SP cells (**Fig. 3F–G**). Under steady-state conditions, rapamycin significantly reduced the frequency of splenic effector memory $CD4^+$ T ($CD44^{hi}CD62L^{lo}$) cells. In contrast, the expression of this T-cell subset was not altered by treatment with aldometanib (**Fig. 3H**). Functionally, aldometanib had subtle effects on $CD4^+$ T-cell IFN-γ production and only mildly suppressed $CD8^+$ T-cell cytokine secretion. In contrast, rapamycin and MK2206 markedly suppressed the secretion of IFN-γ by $CD4^+$ and $CD8^+$ T lymphocytes (**Fig. 3I**). Collectively, these results show that the preliminary safety effect of aldometanib on peripheral immune homeostasis and T-cell development is favoured under our experimental conditions.

Aldometanib Ameliorates Acute Lung Injury and Allergic Lung Inflammation with Altered T-Cell Immune Responses

To determine whether aldometanib alleviates inflammation by inhibiting inflammatory T cell generation, we established an acute lung injury model by

adoptively transferring naive OT-II $CD4^+$ T cells into *Rag1*$^{-/-}$ mice (**Fig. 4A**). Recipient mice were immunized with OVA and subsequently challenged with intranasal OVA from days 8 to 11, which induced robust pulmonary T-cell activation and severe lung injury (**Fig. 4A–C**). Aldometanib treatment markedly attenuated lung damage, preserving alveolar integrity and reducing pulmonary immune cell infiltration (**Fig. 4B–C**). Consistently, aldometanib reduced the $CD4^+$ T-cell proportion, absolute numbers, and IFN-γ secretion in the mediastinal lymph nodes and lung (**Fig. 4D–G**). Aldometanib also diminished the infiltration of innate immune cells into the lung (**Fig. S8A**). To verify the T-cell-intrinsic, AMPK-dependent protective effects of aldometanib, we performed adoptive transfer experiments using WT and *Prkaa1*-KO OT-II Cas9 $CD4^+$ T cells generated via CRISPR-Cas9 gene editing (**Fig. 4H**). The results demonstrated that aldometanib failed to mitigate the lung injury induced by *Prkaa1*-deficient $CD4^+$ T cells and did not affect the pulmonary $CD4^+$ T-cell population, cytokine secretion, or innate immune cell recruitment mediated by *Prkaa1*-KO T cells (**Fig. 4I–K, Fig. S8B**).

We further confirmed these findings in an OVA-induced allergic asthma model (**Fig. S9A**). Aldometanib effectively alleviated airway inflammation and reduced immune cell accumulation in the lymph nodes and lungs (**Fig. S9B-D**). To further clarify whether aldometanib protects against pulmonary inflammation through AMPK in T cells, mixed bone marrow chimeras (BMCs) were generated by adoptive transfer of bone marrow cells into irradiated *Rag1*$^{-/-}$ mice; recipient mice received a 20:80 mixture of bone marrow cells isolated from either WT or *Ampkα1/2*$^{-/-}$;Vav-Cre donors and T-cell-deficient (TCD) mice. In these mixed BMCs, the 20:80 ratio supports the reconstitution of T cells exclusively originating from *Ampkα1/2* KO or WT donors. Eighty percent of the TCD bone marrows sustained near-physiological non-T-cell haematopoietic development, compensating for potential functional defects in non-T-cell populations from 20% of the KO cells. Eight weeks after reconstitution, the mice were challenged with OVA to induce allergic lung inflammation (**Fig. 5A**). The results revealed that aldometanib ameliorated OVA-induced lung injury in WT BMCs; however, the anti-inflammatory efficacy of aldometanib was completely

diminished in KO BMCs (**Fig. 5B**). Moreover, aldometanib failed to inhibit pulmonary infiltration by KO $CD4^+$ T cells or T-cell activation (**Fig. 5C–D**). Consistent with these findings, the ability of aldometanib to suppress cytokine production in Ampk-KO $CD4^+$ T cells was lost, as evidenced by unaltered secretion of IFN-γ, TNF-α, IL-4, and IL-17A (**Fig. 5E**). Moreover, aldometanib had no regulatory effects on Ampk-deficient $CD8^+$ T-cell function or the subsequent accumulation of innate immune cells, which is consistent with comparable IFN-γ/TNF-α secretion and unchanged macrophage and neutrophil numbers in the lungs (**Fig. 5F–G**). Collectively, our results demonstrate that aldometanib alleviates pulmonary inflammation with restraining T-cell activation, expansion and function in an AMPK-dependent manner.

Aldometanib Controls Chronic Colitis by Attenuating Inflammatory T-cell Generation

Aberrant T-cell activation and differentiation are key aspects of chronic gut inflammation pathogenesis; however, effective interventions are still lacking. To evaluate whether aldometanib alleviates chronic colitis, we adoptively transferred naive $CD4^+$ T cells into *Rag1*$^{-/-}$ mice and tracked colitis progression (**Fig. 6A**). The mice in the control group exhibited severe inflammation, including oedema, barrier disruption, and significant immune cell infiltration. Strikingly, aldometanib treatment markedly diminished colon inflammation and immune cell infiltration (**Fig. 6B–E**). Analysis of mLNs and colon-infiltrating T cells revealed decreased T-cell proportions and numbers and significantly reduced IFN-γ, TNF-α, and IL-17A secretion compared with those in the control group (**Fig. 6F–H**), indicating that treatment with aldometanib controls inflammatory T-cell generation in chronic colitis.

Aldometanib may also activate AMPK in other cell types within the colon to regulate intestinal homeostasis. To determine whether aldometanib alleviates colitis via AMPK activation in T cells and/or effects on colon cell homeostasis, we treated *Rag1*$^{-/-}$ mice with either WT or *Ampkα*1/2-KO $CD4^+$ T cells, followed by treatment with aldometanib. Our results demonstrated that aldometanib alleviated colitis

triggered by WT $CD4^+$ T cells in *Rag1*$^{-/-}$ mice, as well as decreased the proportion and absolute number of $CD4^+$ T cells, and reduced the secretion of relevant cytokines. However, these protective effects were markedly diminished following the transfer of KO $CD4^+$ T cells **(Fig. 6I–Q)**. In particular, aldometanib slightly mitigated colitis pathology in *Rag1*$^{-/-}$ mice receiving KO $CD4^+$ T cells (**Fig. 6I–J**), suggesting that aldometanib partially regulates the metabolic homeostasis of diverse cell lineages in the context of chronic colonic inflammation[37]. Overall, these findings suggest that aldometanib relieves colitis by restraining inflammatory T-cell generation and maintaining the internal homeostasis of colonic cells.

Aldometanib Intervention Ameliorates Systemic Lupus Erythematosus Progression in Mice.

SLE is associated not only with intense polyclonal antibody production but also with aberrant T-cell activation and differentiation. Effective T-cell-targeted therapeutics for SLE remain largely unexplored. To elucidate the immunosuppressive effects of aldometanib on SLE progression, we utilized a lupus-prone mouse model (MRL-Fas^{lpr}/J mice). After 3 months of aldometanib treatment, the size and absolute cell numbers of the lymph nodes were significantly reduced in MRL-*lpr* mice (**Fig. 7A–B**). In addition, aldometanib markedly reduced absolute T- and B-cell numbers within the LNs of MRL-*lpr* mice (**Fig. 7B**). Aldometanib treatment also significantly reduced the activation of $CD4^+$ T and $CD8^+$ T cells and decreased the frequency of IFN-γ-secreting T cells (**Fig. 7C-D**). The production of most pathogenic IgG autoantibodies in SLE requires helper signals from $CD4^+$ follicular helper T (Tfh) cells, although T-cell-independent B-cell activation can also contribute to autoantibody generation. We next observed that aldometanib reduced auto-antibody titres in serum, including anti-dsDNA and ANA antibodies as well as plasma cell generation in lupus mice (**Fig. 7E-F**). These results indicated that aldometanib restrains SLE progression, suppressed T-cell function and auto-antibody production.

Lupus nephritis are classic SLE manifestations. A histopathological analysis revealed that aldometanib treatment in MRL-*lpr* mice exhibited improved kidney

morphology and prevented glomerular atrophy (**Fig. 7G**). We also observed that aldometanib reduced glomerular IgG and C3 deposition in the kidneys of lupus mice (**Fig. 7H**). Similarly, aldometanib restored serum C3 levels (**Fig. 7E**) and improved urinary urea and uric acid levels (**Fig. 7I**). Given that urea synthesis and excretion are regulated by the liver and kidney, we further found that aldometanib also normalized serum LDH (**Fig. 7J**), a broad biomarker of cellular damage that may indicate hepatic, renal or other organ injury. Importantly, flow cytometry analysis further demonstrated that cytokine production by kidney-infiltrating T cells was markedly impaired in the aldometanib-treated MRL-*lpr* mice (**Fig. 7K**). Collectively, these results demonstrate that aldometanib effectively attenuates SLE-like disease progression and ameliorates renal injury and associated-biochemical abnormalities in MRL-*lpr* mice. These protective effects are accompanied by reduced inflammatory T cell generation, diminished auto-antibody secretion from plasma cells, and improved renal injury-associated parameters; such benefits are achieved via dual T-cell-dependent and independent regulatory mechanisms.

Aldometanib Reduces Proinflammatory Cytokine Production by T cells in PBMCs from SLE Patients.

To evaluate the function of aldometanib in human autoimmune diseases, we tested the effects of aldometanib on AMPK activation and T-cell function in PBMCs. Our results revealed that among PBMCs from healthy donors, aldometanib clearly increased TCR/CD28-induced AMPK phosphorylation and decreased S6 phosphorylation in human T cells (**Fig. 8A–C**). Consistent with our results observed in mice, aldometanib significantly reduced IFN-γ and TNF-α production by $CD4^+$ T and $CD8^+$ T cells in PBMCs from SLE patients and a subset of healthy donors (**Fig. 8D, 8F, Fig. S10**).

We next used PBMCs isolated from patients with SLE to verify whether the effect of aldometanib on human T cells relies on the AMPK pathway. We evaluated whether compound C, a classic AMPK inhibitor, and Bay3827, a recently developed potent AMPK inhibitor, could reverse aldometanib-mediated T-cell suppression. First, we

observed that treatment with Bay3827 or compound C effectively reversed the aldometanib-mediated reduction in cytokine production by mouse T cells (**Fig. S11**), further demonstrating that the suppression of cytokine secretion by aldometanib is dependent on AMPK activation. Furthermore, aldometanib still suppressed human T-cell function. Treatment with compound C or Bay3827 alone slightly affected T-cell function at the indicated concentration, whereas compound C or Bay3827 treatment with aldometanib largely abrogated the inhibitory effect of aldometanib on cytokine production (**Fig. 8E**). We further performed rescue experiments using a PTEN inhibitor in the same system. Pharmacological inhibition of PTEN also markedly abolished the aldometanib-mediated suppression of cytokine secretion by T cells, consistent with the results obtained using mouse T cells (**Fig. 8E**). Collectively, our findings demonstrate that in SLE PBMCs, aldometanib effectively suppresses human inflammatory T-cell function through an AMPK-dependent pathway and PTEN-associated program.

Discussion

Targeting or modulating T-cell function can alleviate various immune-related diseases, such as SLE, RA, MS, psoriasis, and IBD [38]. Currently, effective clinical strategies, including thymectomy for myasthenia gravis, immunosuppressive therapies using hormones, long-term use of immunosuppressive drug regimens, and B-cell depletion therapies, are well established[39, 40]. Despite these benefits, these approaches carry risks such as immunosuppression, infection, and organ toxicity, which limit their clinical efficacy. Our study revealed that aldometanib inhibits T-cell function by activating AMPK, thus alleviating acute lung inflammation, chronic colitis, and symptoms and kidney injury in a lupus-prone MRL-*lpr* mouse model, and that it has an *ex vivo* inhibitory effect on inflammatory T cells from SLE patients. These findings represent preliminary proof-of-concept evidence.

AMPK is activated under various physiological conditions, such as starvation, stress, and cold. Previous studies have focused primarily on the effects of AMPK activation, often via LKB1 and other signaling pathways, on metabolism and

metabolic diseases. Altered metabolism also attenuates immune responses; for instance, modulating glucose metabolism can suppress immune reactions mainly by inhibiting glycolysis[41]. AMPK activation controls immune responses through fine-tuning metabolic balance; even upstream molecules such as LKB1 directly regulate T-cell differentiation and function, including maintaining Treg-mediated peripheral tolerance and modulating Th17 differentiation[42, 43], whereas SREBP signaling affects Treg function and antitumour immunity[44]. Thus, AMPK activation may have dual metabolic and immunomodulatory functions. Although metformin activates AMPK and regulates blood glucose levels, it acts primarily in the liver, gut, and skeletal muscle; therefore, whether metformin directly modulates T-cell activity still needs to be explored. However, its ability to regulate immune responses *in vivo* suggests that AMPK activation can regulate immune and antitumour responses[45, 46]. The AMPK activator AICAR has therapeutic effects against metabolic diseases and control tumours, and we found that it has a weak modulatory effect on T lymphocytes. Consistent with previous findings, the bioactivity of AICAR is detectable only at elevated concentrations (500 μM to 2 mM)[47, 48]. MK8722, a newly developed AMPK activator, suppresses T-cell function but has been reported to have side effects, such as cardiac hypertrophy, in mice, limiting its long-term use in chronic inflammation[28]. Aldometanib blocks the binding of lysosomal aldolase-FBP to selectively activate lysosomal AMPK. A recent study reported that aldolase depletion leads to lethal metabolic failure and embryonic death [31, 49], and both AMPK activation and aldolase dysfunction may drive metabolic alterations and thereby modulate cell differentiation and function. Aldometanib has been reported to lower blood glucose levels, reduce body weight, alleviate fatty liver disease, and extend lifespan, without causing significant tissue dysfunction or damage. We found that aldometanib inhibited T-cell activation and differentiation to alleviate multiple inflammatory disorders. Importantly, under our experimental conditions, treatment with aldometanib did not cause substantial defects in thymocyte development or peripheral T-cell homeostasis; therefore, it has advantages over treatment with AKT or mTOR inhibitors. Together with our results obtained using clinical PBMC samples,

these data reveal that the preliminary safety profile of aldometanib is favourable in the tested settings, supporting further investigations for potential applications in inflammatory and autoimmune diseases.

Previous studies have reported that AMPK activation suppresses rather than abolishes mTOR activity to maintain cellular homeostasis, consistent with the results of our study. The AKT/mTOR pathway is essential for cell survival and function. However, excessive activation or complete depletion of this pathway can trigger T-cell apoptosis, migratory defects[50, 51], and impaired Treg function[52]. Thus, we propose that aldometanib-mediated AMPK activation enables fine-tuned regulation of AKT/mTOR signaling, which may explain the largely normal thymocyte development and peripheral immune homeostasis but decreased inflammation in diseases upon aldometanib treatment. Although this hypothesis requires further validation, both rapamycin and MK2206 markedly disrupt thymocyte development and the function of peripheral effector T cells.

In addition, our study revealed that AMPK activation modulates PTEN-associated program, as evidenced by the finding that PTEN inhibition completely abrogates the suppressive effect of aldometanib on cytokine production by T cells. PTEN is critical for sustaining cellular homeostasis and function. Loss of PTEN promotes proinflammatory cytokine secretion by T cells or disturbs Treg function[53], via the regulation of the NF-κB, Foxo, ERK, and AKT/mTOR signaling cascades[54-56]. These observations align with our transcriptomic profiling results obtained from aldometanib-treated T cells. Consistent with these findings, a prior study has demonstrated that PTEN can be regulated by metformin-induced AMPK activation [57]. While our data establish the importance of PTEN-associated program for the function of aldometanib, the molecular mechanism through which AMPK activation regulates PTEN-associated program remains poorly defined.

Multiple *in vivo* genetic models, including Ampk-KO T-cell-induced colitis and lung injury and T-cell-specific Ampk-knockout bone marrow chimeras, have consistently demonstrated that the core anti-inflammatory effects of aldometanib depend primarily on AMPK signaling in $CD4^+$ T cells, as evidenced by the

near-complete loss of tissue-protective and cytokine-suppressive capacity in T cells lacking AMPK. However, aldometanib also provides T-cell-independent benefits, such as shielding intestinal epithelial cells[37], and balancing systemic glucose metabolism[31], which together mitigate local inflammatory damage. Our data further revealed that aldometanib has additional therapeutic effects through the regulation of dendritic cells, macrophages, and plasma cells via both T-cell-dependent/independent mechanisms in lung injury, allergic airway inflammation, and MRL/*lpr* lupus mouse models. Supplemental serological and renal biomarkers confirm that it relieves lupus nephritis by restraining pathogenic T-cell responses, lowering autoantibody secretion and restoring tissue homeostasis. We speculate that the anti-inflammatory efficacy and effects of aldometanib on non-T-cell populations may be influenced by drug dosage and treatment period. In our experiments, a lung injury model was treated with aldometanib for 8–17 days, a colitis model was treated for approximately six weeks, and an SLE mouse model was treated for approximately three months. The broad systemic metabolic and immunological benefits of prolonged treatment with aldometanib may also explain its anti-inflammatory effects and lifespan-extending effects[31], and the precise regulatory pathways governing non-T-cell immune subsets remain to be fully characterized.

In summary, this study indicates that aldometanib controls T-cell activation, proliferation and function through AMPK activation and engagement of PTEN-associated programs, significantly alleviating acute and chronic inflammation and autoimmune disease, and offering preliminary proof-of-concept evidence for further investigation of aldometanib as a potential therapeutic strategy for inflammatory and autoimmune diseases.

Limitations of the study

The finding that aldometanib alleviates inflammation and autoimmune diseases by inhibiting inflammatory T-cell generation provides a basis for further research on the broader role of aldometanib in immune diseases. First, aldometanib-mediated suppression of T-cell activation represents a central mechanism underlying its

inhibitory effects on T-cell function. Nevertheless, our current results still cannot fully distinguish a direct effect on Th1/Th17 lineage commitment from secondary effects that arise as a consequence of reduced T-cell activation or proliferation. Second, sustained activation of innate immune cells and B cells can drive diverse inflammatory and autoimmune responses[58]. The effects of aldometanib on innate immune cells and B cells remain to be explored. Moreover, together with existing findings[59], it is not clear whether aldometanib modulates antitumour $CD8^+$ T-cell function and other uncharacterized mechanisms. Third, whether aldometanib directly mediates its anti-inflammatory effects through metabolic reprogramming remains unclear. Notably, aldometanib may perturb the aldolase-FBP glucose-sensing system, and we are therefore unable to fully distinguish the individual contributions of AMPK-dependent signaling and aldolase-related metabolic reprogramming in this study. Previous work has also demonstrated that PTEN and the AKT/mTOR axis serve as key regulators of glycolysis and oxidative phosphorylation, whereas AMPK activation suppresses AKT/mTOR signaling and upregulates PTEN expression[60, 61]. Importantly, how AMPK activation regulates the activity of the PTEN-associated signaling pathway is still unclear. Last, our safety evaluation of aldometanib was limited to the proportions and cell counts of immune cells and T-cell subsets in immune organs. Accordingly, the present data cannot rule out altered immunotoxicity or host defence; thus, further evaluation of general safety, immunotoxicity, and host defence is warranted. Collectively, addressing these limitations represents important directions for future work.

Abbreviations

SLE: systemic lupus erythematosus; PBMCs: peripheral blood mononuclear cells; IBD: inflammatory bowel disease; MS: multiple sclerosis; RA: rheumatoid arthritis; Treg: regulator T cell; AMPK: AMP-activated protein kinase; OVA-OT-II system: OVA/dendritic cell (DC)-stimulated OT-II cell activation model; LNs: lymph nodes; mLNs: mesenteric lymph nodes.

Supplementary Material

Supplementary methods, figures and tables.

Data and code availability

All RNA-seq raw sequences have been deposited to the NCBI Sequence Read Archive under BioProject accession PRJNA1370081. Researchers may contact the corresponding lead author to obtain extra raw data and analytical scripts required to replicate our analyses.

Acknowledgements

We appreciate all patients who generously provided their PBMCs for this study. This work was financially supported by the National Natural Science Foundation of China (82202006 to C.L. and 32470978， 32070877 to W-H. L.), Key Project of Natural Science Research of Anhui Education Department (2022AH050778), Incubation Project of Xiang'an Innovation Laboratory (2023XAKJ0101035 to W-H.L.). Generative-AI tool (ChatGPT-4, OpenAI) was used solely for English-language editing, grammatical correction and improvement of textual readability during manuscript preparation. The authors fully reviewed and edited all AI-assisted content. No AI tools were applied for data collection, data analysis or image manipulation, and the authors take full responsibility for the integrity and content of this manuscript.

Author contributions

C. L. C.Z and W-H.L. designed the experiments. C.L, Y.Z., F.W and T.W. performed most of the experiments. Y.Z. analyzed the data. R.H., M.Z., C.D. helped with animal studies and HE staining. X.H., X.W., K.Z., L.F. helped with *in vitro* experiments. Y.W and Y.H. performed immune blot assays. Z.F analyzed the RNA-seq data and biostatistical analysis. Y.H. and Y.Z. provided patient samples and analyzed the data for the project. C.L., W-H.L., Y.W and Z.F. wrote the manuscript, C.L., W-H.L. and F.Z. provided funding support.

Declaration of interests

The authors declare no competing interests.

Reference

1. Zhang R, Zhao Y, Chen X, Zhuang Z, Li X, Shen E. Low-dose IL-2 therapy in autoimmune diseases: An update review. Int Rev Immunol. 2024; 43: 113-37.
2. Dong C. Cytokine Regulation and Function in T Cells. Annu Rev Immunol. 2021; 39: 51-76.
3. Zarrin AA, Bao K, Lupardus P, Vucic D. Kinase inhibition in autoimmunity and inflammation. Nat Rev Drug Discov. 2021; 20: 39-63.
4. Scherlinger M, Kolios AGA, Kyttaris VC, Tsokos GC. Advances in the treatment of systemic lupus erythematosus. Nat Rev Drug Discov. 2025; 24: 926-44.
5. Bonelli M, Kerschbaumer A, Kastrati K, Ghoreschi K, Gadina M, Heinz LX, et al. Selectivity, efficacy and safety of JAKinibs: new evidence for a still evolving story. Ann Rheum Dis. 2024; 83: 139-60.
6. Hoffmann MH, Kirchner H, Krönke G, Riemekasten G, Bonelli M. Inflammatory tissue priming: novel insights and therapeutic opportunities for inflammatory rheumatic diseases. Ann Rheum Dis. 2024; 83: 1233-53.
7. Huang H, Long L, Zhou P, Chapman NM, Chi H. mTOR signaling at the crossroads of environmental signals and T-cell fate decisions. Immunol Rev. 2020; 295: 15-38.
8. Solinas G, Becattini B. PI3K and AKT at the Interface of Signaling and Metabolism. Curr Top Microbiol Immunol. 2022; 436: 311-36.
9. Zhang X, Jia L, Lin X, Zhou L. The FOXO1-SIRT1 axis in ankylosing spondylitis: A cross-platform regulator linking immunometabolism, oxidative stress, and bone remodeling. Autoimmun Rev. 2025; 24: 103878.
10. Pandit M, Timilshina M, Chang JH. LKB1-PTEN axis controls Th1 and Th17 cell differentiation via regulating mTORC1. J Mol Med (Berl). 2021; 99: 1139-50.
11. Charbonnier LM, Cui Y, Stephen-Victor E, Harb H, Lopez D, Bleesing JJ, et al. Functional reprogramming of regulatory T cells in the absence of Foxp3. Nat Immunol. 2019; 20: 1208-19.
12. Shen H, Ojo OA, Ding H, Mullen LJ, Xing C, Hossain MI, et al. HIF1α-regulated glycolysis promotes activation-induced cell death and IFN-γ induction in hypoxic T cells. Nat Commun. 2024; 15: 9394.
13. Dang EV, Barbi J, Yang HY, Jinasena D, Yu H, Zheng Y, et al. Control of T(H)17/T(reg) balance by hypoxia-inducible factor 1. Cell. 2011; 146: 772-84.
14. Lin Y, Zhu X, Li Y, Dou Y, Wang J, Qi R, et al. LY294002 ameliorates psoriatic skin inflammation in mice via blocking the Notch1/Hes1-PTEN/AKT/IL-17A feedback loop. Clin Exp Immunol. 2023; 213: 114-24.
15. Hou H, Cao R, Miao J, Sun Y, Liu X, Song X, et al. Fingolimod ameliorates the development of experimental autoimmune encephalomyelitis by inhibiting Akt-mTOR axis in mice. Int Immunopharmacol. 2016; 30: 171-8.
16. Paskiewicz A, Niu J, Chang C. Autoimmune lymphoproliferative syndrome: A disorder of immune dysregulation. Autoimmun Rev. 2023; 22: 103442.
17. Su TI, Khanna D, Furst DE, Danovitch G, Burger C, Maranian P, et al. Rapamycin versus methotrexate in early diffuse systemic sclerosis: results from a randomized, single-blind pilot study. Arthritis Rheum. 2009; 60: 3821-30.
18. Hirayama Y, Gi M, Yamano S, Tachibana H, Okuno T, Tamada S, et al. Anti-PD-L1 treatment enhances antitumor effect of everolimus in a mouse model of renal cell carcinoma. Cancer Sci. 2016; 107: 1736-44.
19. Yap TA, Yan L, Patnaik A, Fearen I, Olmos D, Papadopoulos K, et al. First-in-man clinical trial

of the oral pan-AKT inhibitor MK-2206 in patients with advanced solid tumors. J Clin Oncol. 2011; 29: 4688-95.
20. Gonzalez-Angulo AM, Meric-Bernstam F, Chawla S, Falchook G, Hong D, Akcakanat A, et al. Weekly nab-Rapamycin in patients with advanced nonhematologic malignancies: final results of a phase I trial. Clin Cancer Res. 2013; 19: 5474-84.
21. Lin SC, Hardie DG. AMPK: Sensing Glucose as well as Cellular Energy Status. Cell Metab. 2018; 27: 299-313.
22. González A, Hall MN, Lin SC, Hardie DG. AMPK and TOR: The Yin and Yang of Cellular Nutrient Sensing and Growth Control. Cell Metab. 2020; 31: 472-92.
23. Ma T, Tian X, Zhang B, Li M, Wang Y, Yang C, et al. Low-dose metformin targets the lysosomal AMPK pathway through PEN2. Nature. 2022; 603: 159-65.
24. Owen MR, Doran E, Halestrap AP. Evidence that metformin exerts its anti-diabetic effects through inhibition of complex 1 of the mitochondrial respiratory chain. Biochem J. 2000; 348 Pt 3: 607-14.
25. Cha JH, Yang WH, Xia W, Wei Y, Chan LC, Lim SO, et al. Metformin Promotes Antitumor Immunity via Endoplasmic-Reticulum-Associated Degradation of PD-L1. Mol Cell. 2018; 71: 606-20.e7.
26. Graham GG, Punt J, Arora M, Day RO, Doogue MP, Duong JK, et al. Clinical pharmacokinetics of metformin. Clin Pharmacokinet. 2011; 50: 81-98.
27. Hunter RW, Hughey CC, Lantier L, Sundelin EI, Peggie M, Zeqiraj E, et al. Metformin reduces liver glucose production by inhibition of fructose-1-6-bisphosphatase. Nat Med. 2018; 24: 1395-406.
28. Myers RW, Guan HP, Ehrhart J, Petrov A, Prahalada S, Tozzo E, et al. Systemic pan-AMPK activator MK-8722 improves glucose homeostasis but induces cardiac hypertrophy. Science. 2017; 357: 507-11.
29. Višnjić D, Lalić H, Dembitz V, Tomić B, Smoljo T. AICAr, a Widely Used AMPK Activator with Important AMPK-Independent Effects: A Systematic Review. Cells. 2021; 10.
30. Olivier S, Foretz M, Viollet B. Promise and challenges for direct small molecule AMPK activators. Biochem Pharmacol. 2018; 153: 147-58.
31. Zhang CS, Li M, Wang Y, Li X, Zong Y, Long S, et al. The aldolase inhibitor aldometanib mimics glucose starvation to activate lysosomal AMPK. Nat Metab. 2022; 4: 1369-401.
32. Liu Q, Zhou Y, Ma L, Gu F, Liao K, Liu Y, et al. Sulfate oligosaccharide of Gracilaria lemaneiformis modulates type 1 immunity by restraining T cell activation. Carbohydr Polym. 2022; 288: 119377.
33. Ma Z, Zhou Y, Gu F, Wu F, Hong Y, Liu WH, et al. Berberine alleviates T cell-driven lung inflammation by inhibiting cytokine secretion and regulating pulmonary microbiota. Biochem Biophys Res Commun. 2025; 778: 152390.
34. Liu WH, Kang SG, Huang Z, Wu CJ, Jin HY, Maine CJ, et al. A miR-155-Peli1-c-Rel pathway controls the generation and function of T follicular helper cells. J Exp Med. 2016; 213: 1901-19.
35. Zhang C, Tam TW, Chau MK, García Córdoba CA, Yung S, Chan TM. Effect of Combined Mycophenolate and Rapamycin Treatment on Kidney Fibrosis in Murine Lupus Nephritis. Front Pharmacol. 2022; 13: 866077.
36. Tang YQ, Li ZW, Feng YF, Yang HQ, Hou CL, Geng C, et al. MK2206 attenuates atherosclerosis by inhibiting lipid accumulation, cell migration, proliferation, and inflammation. Acta Pharmacol Sin. 2022; 43: 897-907.

948 37. Olivier S, Diounou H, Pochard C, Frechin L, Durieu E, Foretz M, et al. Intestinal Epithelial
949 AMPK Deficiency Causes Delayed Colonic Epithelial Repair in DSS-Induced Colitis. Cells. 2022; 11.
950 38. Sun L, Su Y, Jiao A, Wang X, Zhang B. T cells in health and disease. Signal Transduct Target
951 Ther. 2023; 8: 235.
952 39. Cooper JD. History of Thymectomy for Myasthenia Gravis. Thorac Surg Clin. 2019; 29: 151-8.
953 40. Chung JB, Brudno JN, Borie D, Kochenderfer JN. Chimeric antigen receptor T cell therapy for
954 autoimmune disease. Nat Rev Immunol. 2024; 24: 830-45.
955 41. Peng M, Yin N, Chhangawala S, Xu K, Leslie CS, Li MO. Aerobic glycolysis promotes T helper
956 1 cell differentiation through an epigenetic mechanism. Science. 2016; 354: 481-4.
957 42. Yang K, Blanco DB, Neale G, Vogel P, Avila J, Clish CB, et al. Homeostatic control of metabolic
958 and functional fitness of T(reg) cells by LKB1 signalling. Nature. 2017; 548: 602-6.
959 43. Baixauli F, Piletic K, Puleston DJ, Villa M, Field CS, Flachsmann LJ, et al. An
960 LKB1-mitochondria axis controls T(H)17 effector function. Nature. 2022; 610: 555-61.
961 44. Lim SA, Wei J, Nguyen TM, Shi H, Su W, Palacios G, et al. Lipid signalling enforces functional
962 specialization of T(reg) cells in tumours. Nature. 2021; 591: 306-11.
963 45. Bharath LP, Agrawal M, McCambridge G, Nicholas DA, Hasturk H, Liu J, et al. Metformin
964 Enhances Autophagy and Normalizes Mitochondrial Function to Alleviate Aging-Associated
965 Inflammation. Cell Metab. 2020; 32: 44-55.e6.
966 46. Finisguerra V, Dvorakova T, Formenti M, Van Meerbeeck P, Mignion L, Gallez B, et al.
967 Metformin improves cancer immunotherapy by directly rescuing tumor-infiltrating CD8 T
968 lymphocytes from hypoxia-induced immunosuppression. J Immunother Cancer. 2023; 11.
969 47. Rao E, Zhang Y, Li Q, Hao J, Egilmez NK, Suttles J, et al. AMPK-dependent and independent
970 effects of AICAR and compound C on T-cell responses. Oncotarget. 2016; 7: 33783-95.
971 48. Blagih J, Coulombe F, Vincent EE, Dupuy F, Galicia-Vázquez G, Yurchenko E, et al. The energy
972 sensor AMPK regulates T cell metabolic adaptation and effector responses in vivo. Immunity. 2015; 42:
973 41-54.
974 49. Koscielny G, Yaikhom G, Iyer V, Meehan TF, Morgan H, Atienza-Herrero J, et al. The
975 International Mouse Phenotyping Consortium Web Portal, a unified point of access for knockout mice
976 and related phenotyping data. Nucleic Acids Res. 2014; 42: D802-9.
977 50. White TLA, Jin Y, Gable MJ, Morel PA. Recent insights into the role of Akt in CD4 T-cell
978 activation and differentiation: alternative splicing and beyond. Immunometabolism (Cobham). 2023; 5:
979 e00015.
980 51. Liu C, Ma L, Wang Y, Zhao J, Chen P, Chen X, et al. Glycogen synthase kinase 3 drives
981 thymocyte egress by suppressing β-catenin activation of Akt. Sci Adv. 2021; 7: eabg6262.
982 52. Zeng H, Yang K, Cloer C, Neale G, Vogel P, Chi H. mTORC1 couples immune signals and
983 metabolic programming to establish T(reg)-cell function. Nature. 2013; 499: 485-90.
984 53. Shrestha S, Yang K, Guy C, Vogel P, Neale G, Chi H. Treg cells require the phosphatase PTEN
985 to restrain TH1 and TFH cell responses. Nat Immunol. 2015; 16: 178-87.
986 54. Tian Y, Li H, Qiu T, Dai J, Zhang Y, Chen J, et al. Loss of PTEN induces lung fibrosis via
987 alveolar epithelial cell senescence depending on NF-κB activation. Aging Cell. 2019; 18: e12858.
988 55. Blanco DB, Chapman NM, Raynor JL, Xu C, Su W, Kc A, et al. PTEN directs developmental
989 and metabolic signaling for innate-like T cell fate and tissue homeostasis. Nat Cell Biol. 2022; 24:
990 1642-54.
991 56. Pasha A, Kumar K, Heena SK, Arnold Emerson I, Pawar SC. Inhibition of NF-kB and COX-2 by

andrographolide regulates the progression of cervical cancer by promoting PTEN expression and suppressing PI3K/AKT signalling pathway. Sci Rep. 2024; 14: 12020.

57. Kim SA, Choi HC. Metformin inhibits inflammatory response via AMPK-PTEN pathway in vascular smooth muscle cells. Biochem Biophys Res Commun. 2012; 425: 866-72.

58. Meng X, Asadi-Asadabad S, Cao S, Song R, Lin Z, Safhi M, et al. Metabolic rewiring controlled by HIF-1α tunes IgA-producing B-cell differentiation and intestinal inflammation. Cell Mol Immunol. 2025; 22: 54-67.

59. Hu HH, Wang X, Lan B, Cheng H, Wen H, Chen F, et al. Glucose starvation mimetic aldometanib removes immune barriers permitting mice with hepatocellular carcinoma to live to normal ages. Cell Res. 2025; 35: 934-53.

60. Cheng SC, Quintin J, Cramer RA, Shepardson KM, Saeed S, Kumar V, et al. mTOR- and HIF-1α-mediated aerobic glycolysis as metabolic basis for trained immunity. Science. 2014; 345: 1250684.

61. Qian X, Li X, Shi Z, Xia Y, Cai Q, Xu D, et al. PTEN Suppresses Glycolysis by Dephosphorylating and Inhibiting Autophosphorylated PGK1. Mol Cell. 2019; 76: 516-27.e7.

Figures

Graphical Abstract

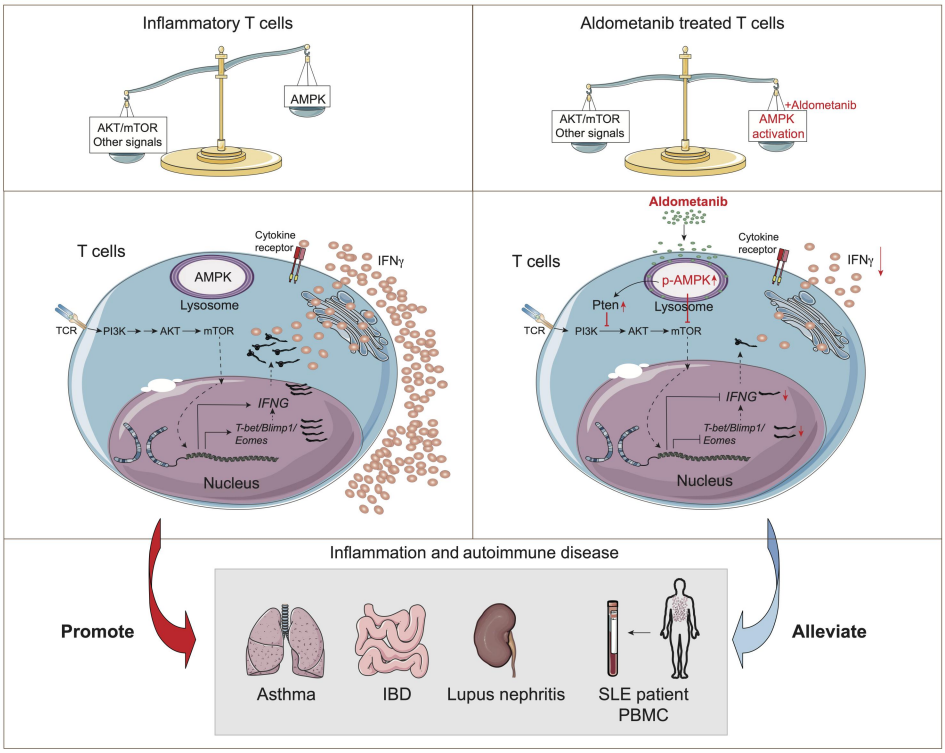

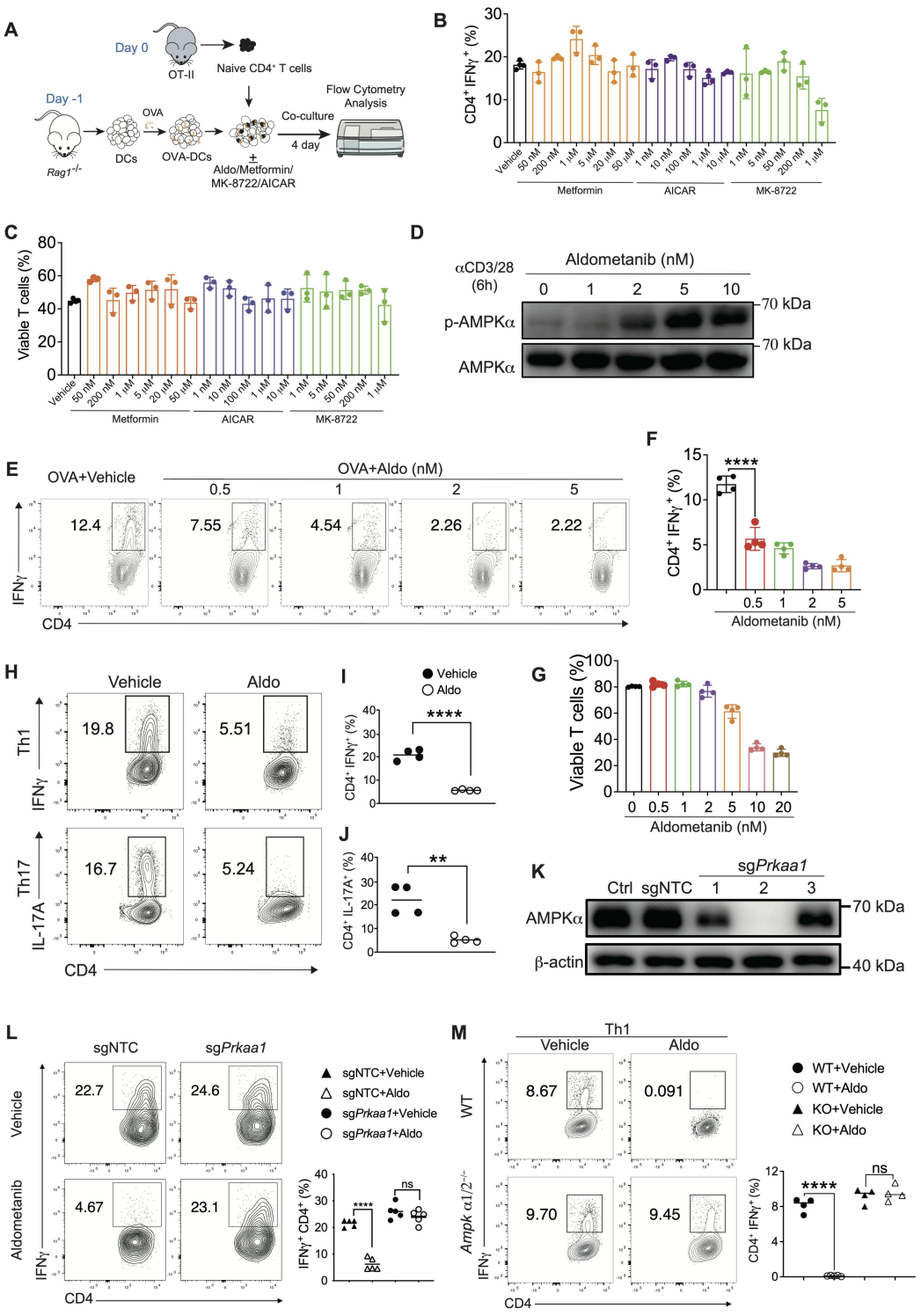

Fig. 1. Aldometanib activates AMPK in T cells to suppress proinflammatory cytokine production.

(A) Model of the OVA-OT-II system. (B and C) IFNγ production and cell viability of $CD4^+$ T cells treated with metformin, AICAR or MK-8722 (n ⩾ 3 per group). (D) Immunoblot detection of phosphorylated AMPK in $CD4^+$ T cells incubated with 0, 1, 2, 5, or 10 nM aldometanib for 6 h. (E-G) IFNγ secretion and cell viability of $CD4^+$ T cells with aldometanib treatment (n = 4). (H-J) Th1 (H, I) and Th17 polarization (H, J) following aldometanib treatment (n = 4 per group). (K) AMPK expression in sg*Prkaa1*-edited OT-II $CD4^+$ T cells. (L) Flow cytometric analysis of 2 nM

aldometanib-mediated IFNγ secretion in sg*Prkaa1*-knockout CD4$^+$ T cells *in vitro* (n=5). (M) Effects of 2 nM aldometanib on Th1 differentiation in WT and AMPKα1/2$^{-/-}$ (*Ampk*α1/2$^{fl/fl}$;Vav Cre) CD4$^+$ T cells (n ⩾ 4).

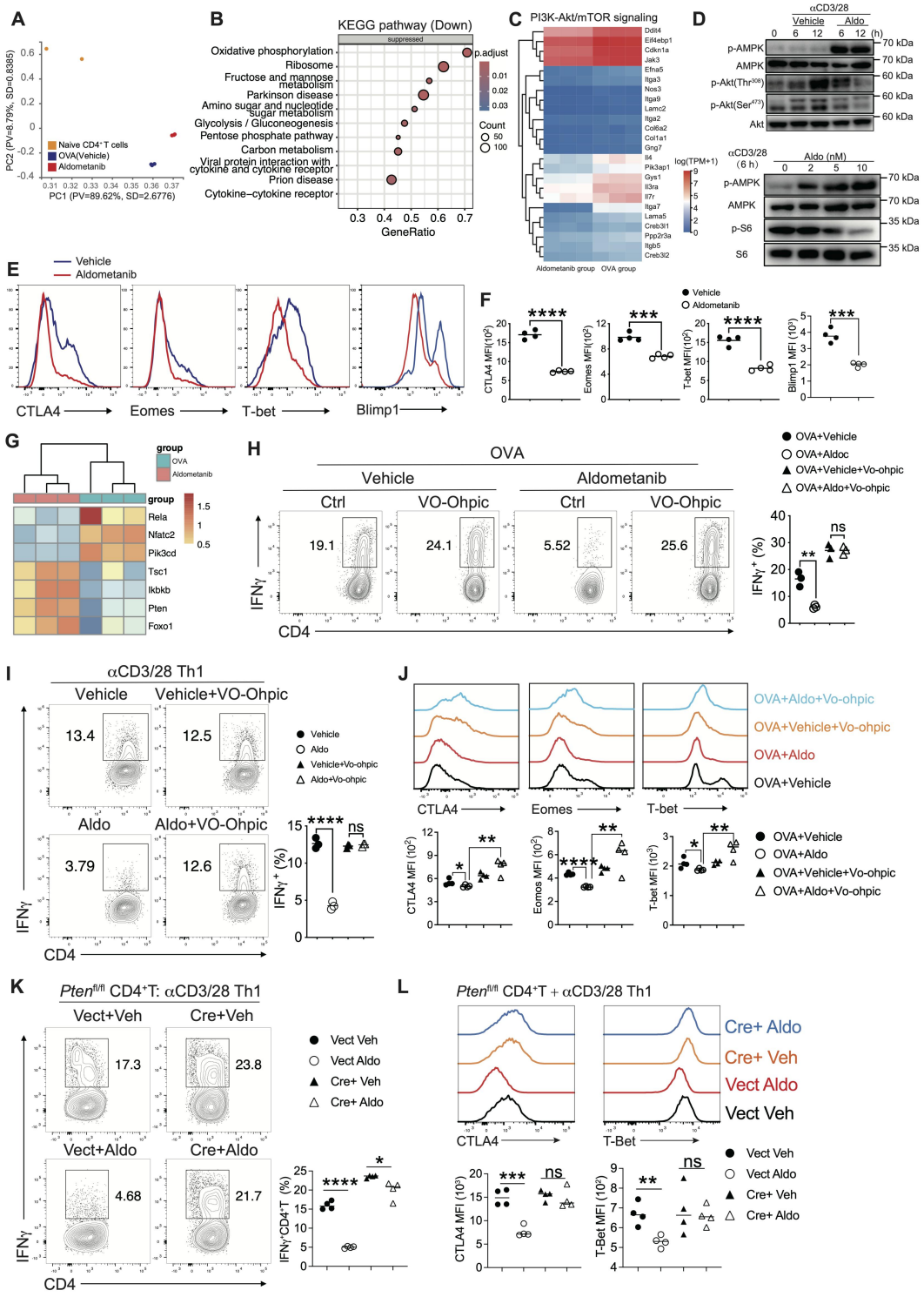

Fig. 2. Aldometanib regulates T cell function via AKT/mTOR activity and PTEN-associated programs.

(A) PCA plot of RNA-seq. (B) KEGG analysis of downregulated genes in 2nM aldometanib-treated CD4$^+$ T cells. (C) Decreased PI3K-Akt signaling pathway after aldometanib

treatment. (D) Immunoblot analysis WT $CD4^+$ T cells stimulated by anti-CD3/CD28. Top panel: phosphorylation levels of Akt and AMPK in T cells treated with 2 nM aldometanib for 6 h or 12 h. Bottom panel: phosphorylated S6 ribosomal protein and AMPK activation in T cells incubated with 0, 2, 5, or 10 nM aldometanib for 6 h. (E, F) Expression of Eomes, T-bet, Blimp1 and CTLA-4 in aldometanib-treated $CD4^+$ T cells (n = 4). (G) RNA-Seq analysis of the *Pten* and *Foxo1* expression in $CD4^+$ T cells following aldometanib treatment. (H, I) IFN-γ secretion from 2nM aldometanib-treated T cells with or without 10 μM VO-Ohpic intervention; cells were stimulated via the OVA-OT-II system (H) or anti-CD3/CD28 co-stimulation (I) (n = 3). (J) Expression of Eomes, T-bet, Blimp1 and CTLA-4 in 2nM aldometanib-treated OT-II $CD4^+$ T cells with 10 μM VO-Ohpic co-treatment (n=4). (K, L) Flow cytometric quantification of IFN-γ production (K) and CTLA-4/T-bet expression (L) in $Pten^{fl/fl}$ $CD4^+$ T cells transduced with Cre recombinase or empty vector, followed by incubation with 2nM Aldometanib or vehicle control. Cells were cultured under in vitro Th1-polarizing conditions with anti-CD3/CD28 stimulation (n=4) .

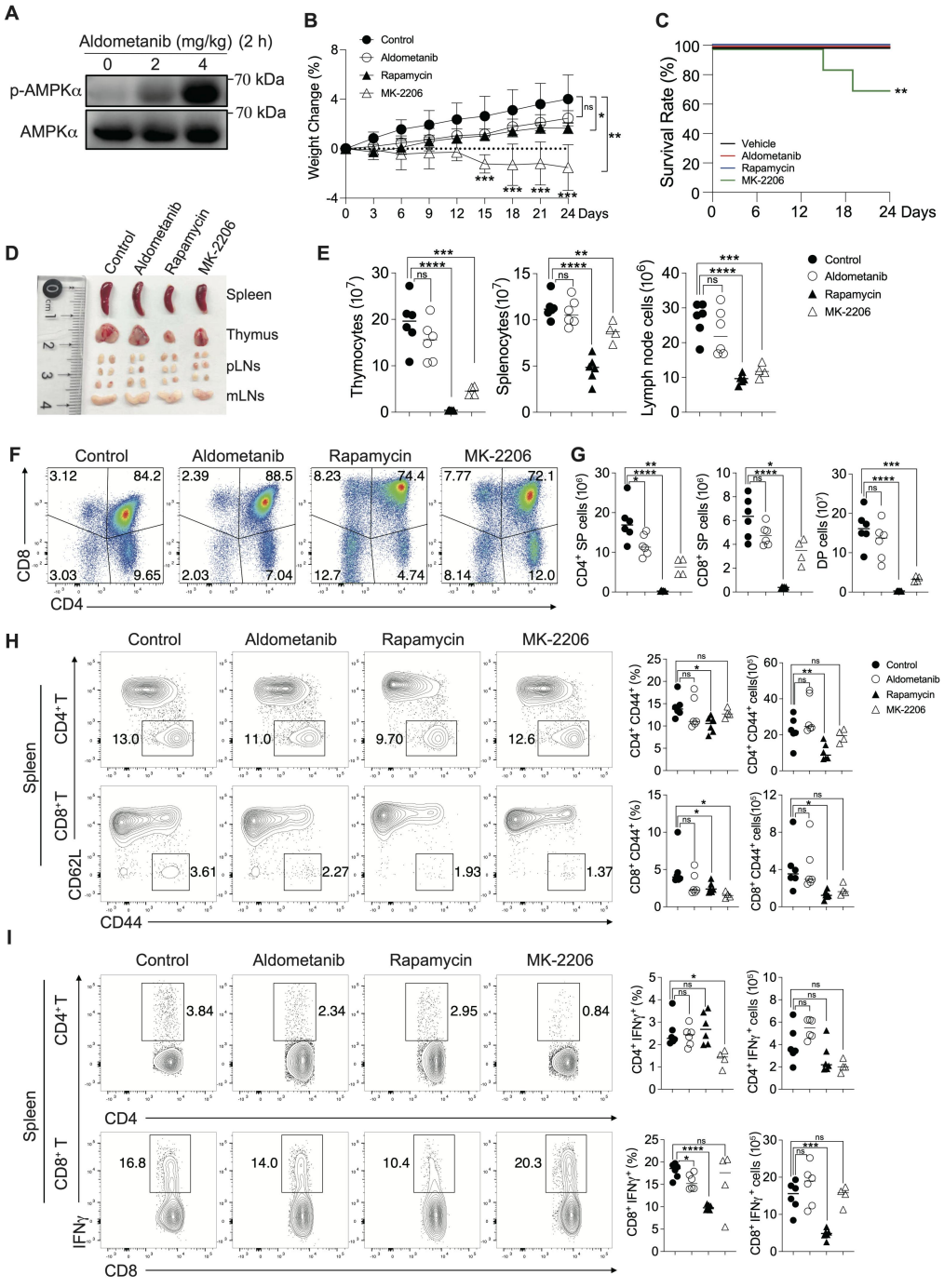

Fig. 3. Aldometanib Shows Favorable Preliminary Safety in Peripheral Immune Homeostasis and T-cell Development

(A) Phosphorylated AMPK (p-AMPK) expression in mouse lymph nodes harvested 2 h after oral administration of aldometanib. (B-D) Changes in mouse body weight (B), survival (C), and immune organ morphology (D) following treatment with aldometanib, rapamycin or MK-2206 (n ≥ 4 per group). (E) Total cell counts in central (thymus) and peripheral (spleen, lymph nodes) immune organs from mice treated with aldometanib, rapamycin or MK-2206 (n≥4). (F, G) T cell developmental subsets in mice treated with aldometanib, rapamycin or MK-2206 (n ≥ 4). (H, I) T cell activation (H) and IFN-γ secretion (I) in splenic $CD4^+$ (top panels) and $CD8^+$ T cells (bottom panels) (n ≥ 4). Body weight changes were analyzed using one-way ANOVA followed by Tukey's

HSD post-hoc test for multiple comparisons. Survival data were analyzed by the Kaplan-Meier method with the log-rank test for intergroup comparisons.

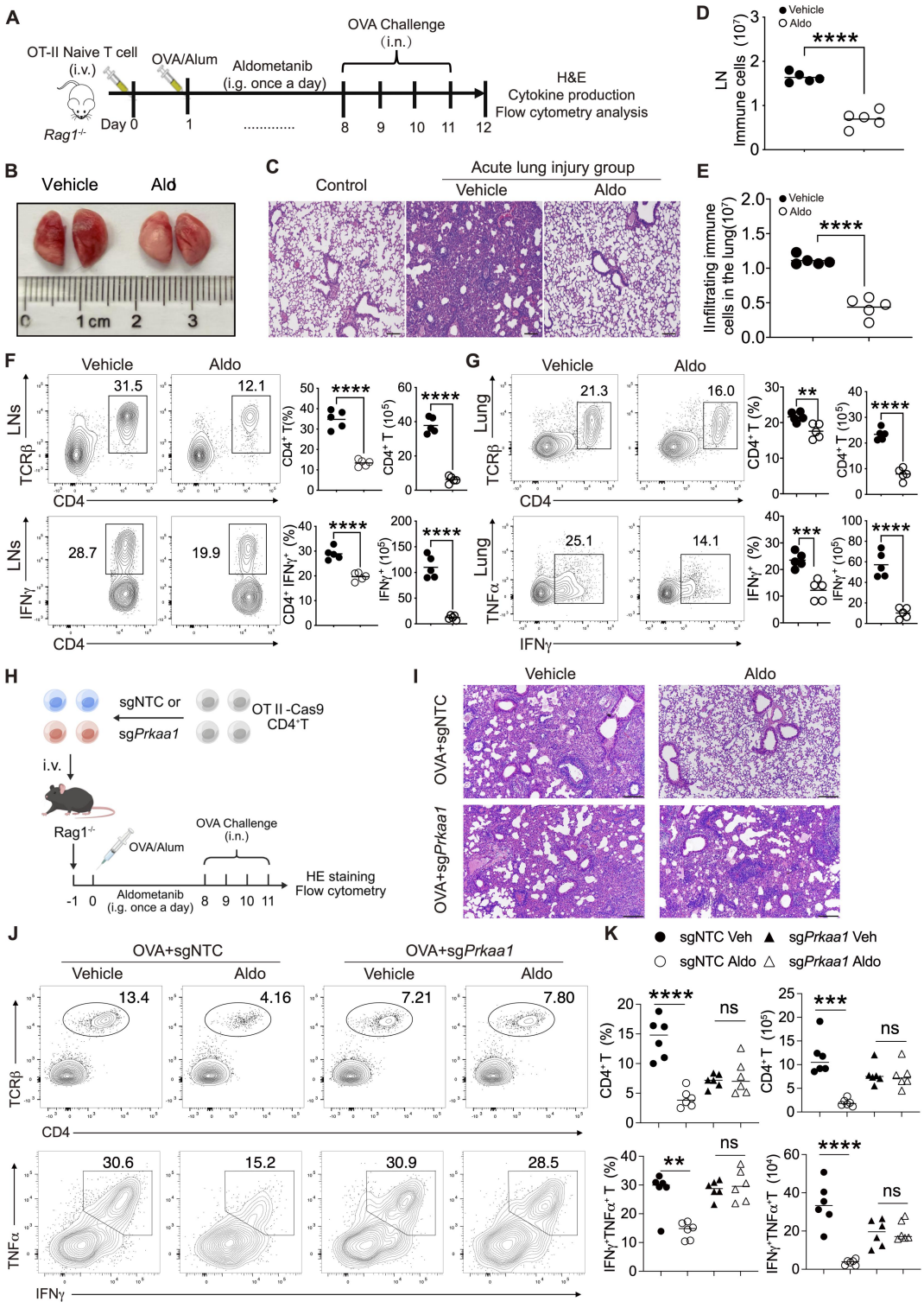

Fig. 4. Aldometanib alleviates acute lung injury with restraining T cell function in an AMPK-dependent manner.

(A) Schematic illustration of the $CD4^+$ T cell-induced acute lung injury model. (B, C) Gross lung phenotypes (B) and lung H&E staining (C) of mice with or without aldometanib treatment in the

model shown in (A). Scale bar, 200 μm. (D, E) Infiltrated immune cell numbers in lymph nodes (D) and lung tissue (E) from the above model (n = 5). (F, G) $CD4^+$ T cell subsets and cytokine production (IFN-γ) in lymph nodes (F) and lung tissue (G) (n = 5 per group). (H) Schematic of acute lung injury established via adoptive transfer of *Prkaa1*-deficient OT-II-Cas9 $CD4^+$ T cells. (I) Representative images of lung tissue from the (H) with or without aldometanib treatment. Scale bar, 200 μm. (J, K) Percentage and numbers of $CD4^+$ T cells and IFN-γ^+ TNF-α^+ $CD4^+$T cells infiltrating the lung under model (H) (n = 6).

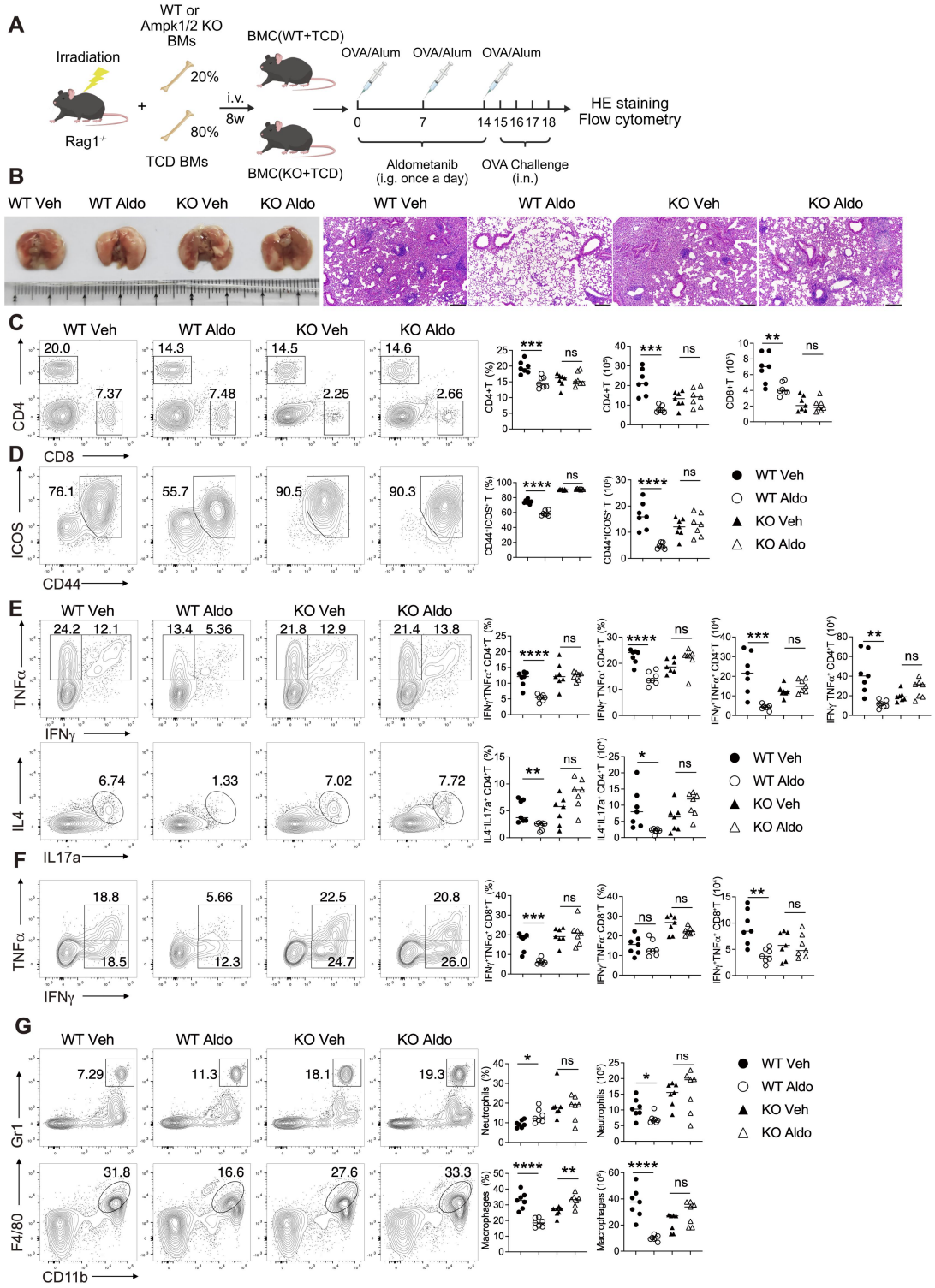

Fig. 5. Aldometanib alleviates allergic lung inflammation with impaired T cell function in an AMPK-dependent manner.

(A) Schematic diagram for generating bone marrow chimeras with T cell specific deletion of AMPKα1/2 (named WT or KO), followed by OVA induced allergic lung inflammation. (B) Gross lung appearance and representative lung H&E staining of mice with or without aldometanib treatment in WT or KO mice. Scale bar, 200 μm. (C, D) Flow cytometric quantification of WT and Ampkα1/2-deficient T cell percentages (C), and activated $CD4^+$ T cells ($CD44^+$ $ICOS^+$) (D) isolated from lung (n=7 per group). (E, F) Flow cytometric detection of cytokine production in lung-infiltrated WT and Ampkα1/2-deficient T cells: $CD4^+$ T cells (IFN-γ^+TNF-α^+, IL-4^+IL-$17a^+$) (E) and $CD8^+$ T cells (IFN-γ^+TNF-α^+) (F) (n = 7). (G) Quantification of macrophages and neutrophils in lung with/without aldometanib treatment (n = 7 per group).

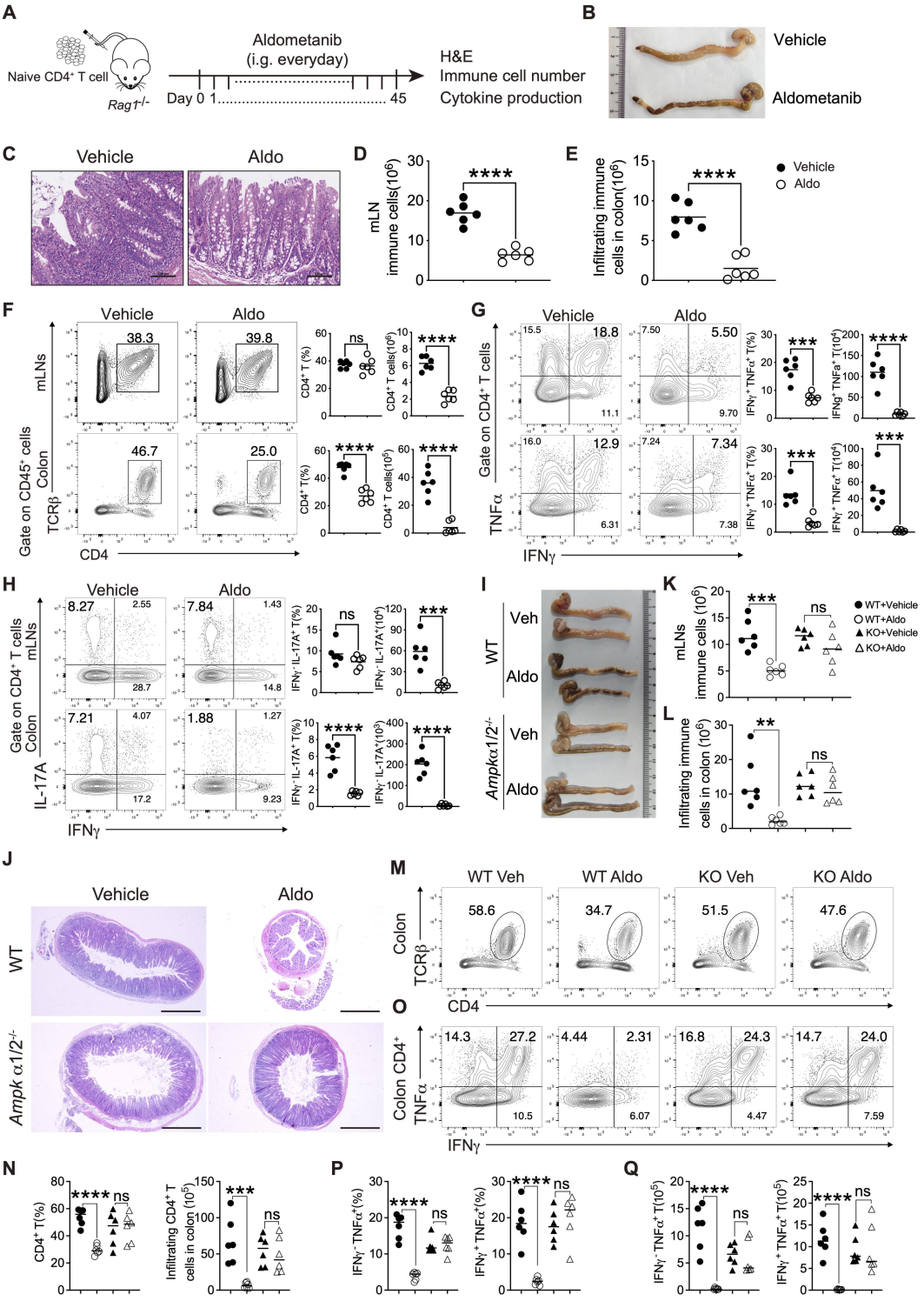

Fig. 6. Aldometanib mitigates colitis by suppressing inflammatory T cell generation.

(A) Schematic illustration of the CD4$^+$ T cell-induced chronic colitis. (B, C) Gross colorectal morphology and representative H&E images of colon in indicated group. Scale bar, 100 μm. (D, E) Quantification of infiltrated immune cells in mLNs (D) and colorectal tissues (E) (n = 6). (F–H) CD4$^+$ T cell proportions (F) and secretion of IFN-γ, TNF-α, and IL-17A (G, H) in mLNs and colon (n = 6). (I, J) Gross colorectal appearance (I) and representative colorectal H&E staining (J) from WT or Ampkα1/2$^{-/-}$ CD4$^+$ T cell induced colitis and treated with aldometanib or vehicle. Scale bar, 1 mm. (K, L) Quantification of infiltrated immune cells in mesenteric lymph nodes (K)

and colon (L) isolated from mice of WT or Ampkα1/2$^{-/-}$ CD4$^+$ T cell group (n = 6 per group). (M–Q) Flow cytometric detection of CD4$^+$ T cell populations (M, N) and IFN-γ$^+$/TNF-α$^+$ cytokine production (O-Q) in colon from mice of WT or Ampkα1/2$^{-/-}$ CD4$^+$ T cell group (n = 6 per group).

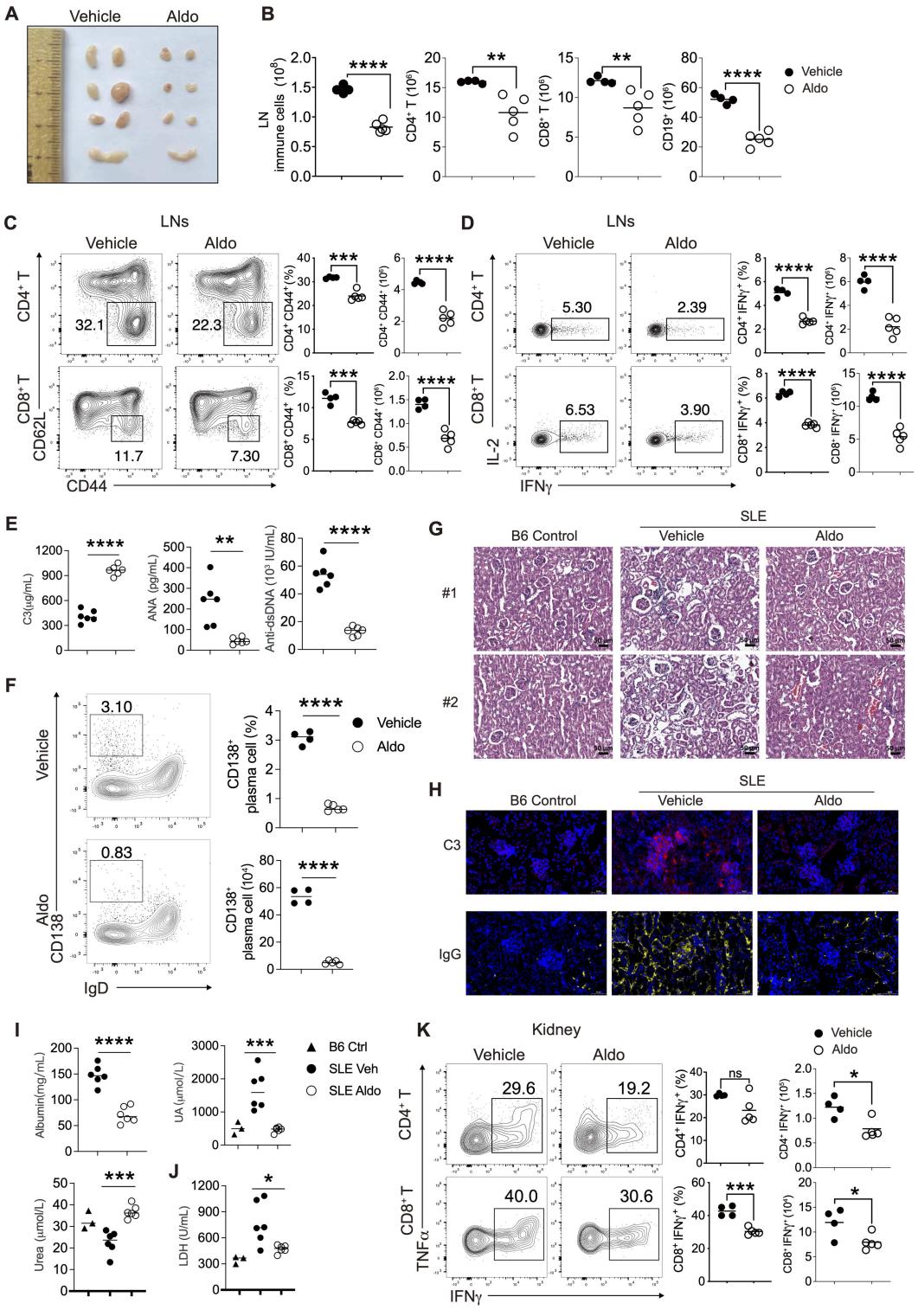

Fig. 7. Aldometanib intervention ameliorates systemic lupus erythematosus progression. (A) Representative lymph nodes histopathology from vehicle or aldometanib-treated MRL-*lpr* mice. (B) Quantification of total lymph node cellularity and the proportions of CD4$^+$ and CD8$^+$ T

cells and B cells in MRL-*lpr* mice with or without aldometanib treatment ($n \geq 4$ per group). (C, D) T cell activation (C) and IFN-γ secretion (D) of $CD4^+$ and $CD8^+$ T cells in lymph nodes ($n \geq 4$). (E) Serum concentrations of complement C3, ANA and anti-dsDNA autoantibodies in MRL-*lpr* mice following aldometanib administration ($n = 6$). (F) Flow cytometric quantification of plasma cell populations in LNs in aldometanib treated MRL-*lpr* mice ($n \geq 4$). (G) H&E images of renal tissues from MRL-*lpr* mice treated with vehicle or aldometanib. Scale bar, 50 μm. (H) C3 (red) and IgG (yellow) depositions were shown via immunofluorescence staining in the kidneys of aldometanib-treated MRL-*lpr* mice. Scale bar, 50 μm. (I,J) Urinary levels of albumin, uric acid (UA), urea (I) and serum LDH (J)in MRL-*lpr* mice after aldometanib intervention ($n \geq 3$ per group). (K) Flow cytometric detection of cytokine secretion by kidney-infiltrating T cells in aldometanib treated MRL-*lpr* mice ($n \geq 4$ per group).

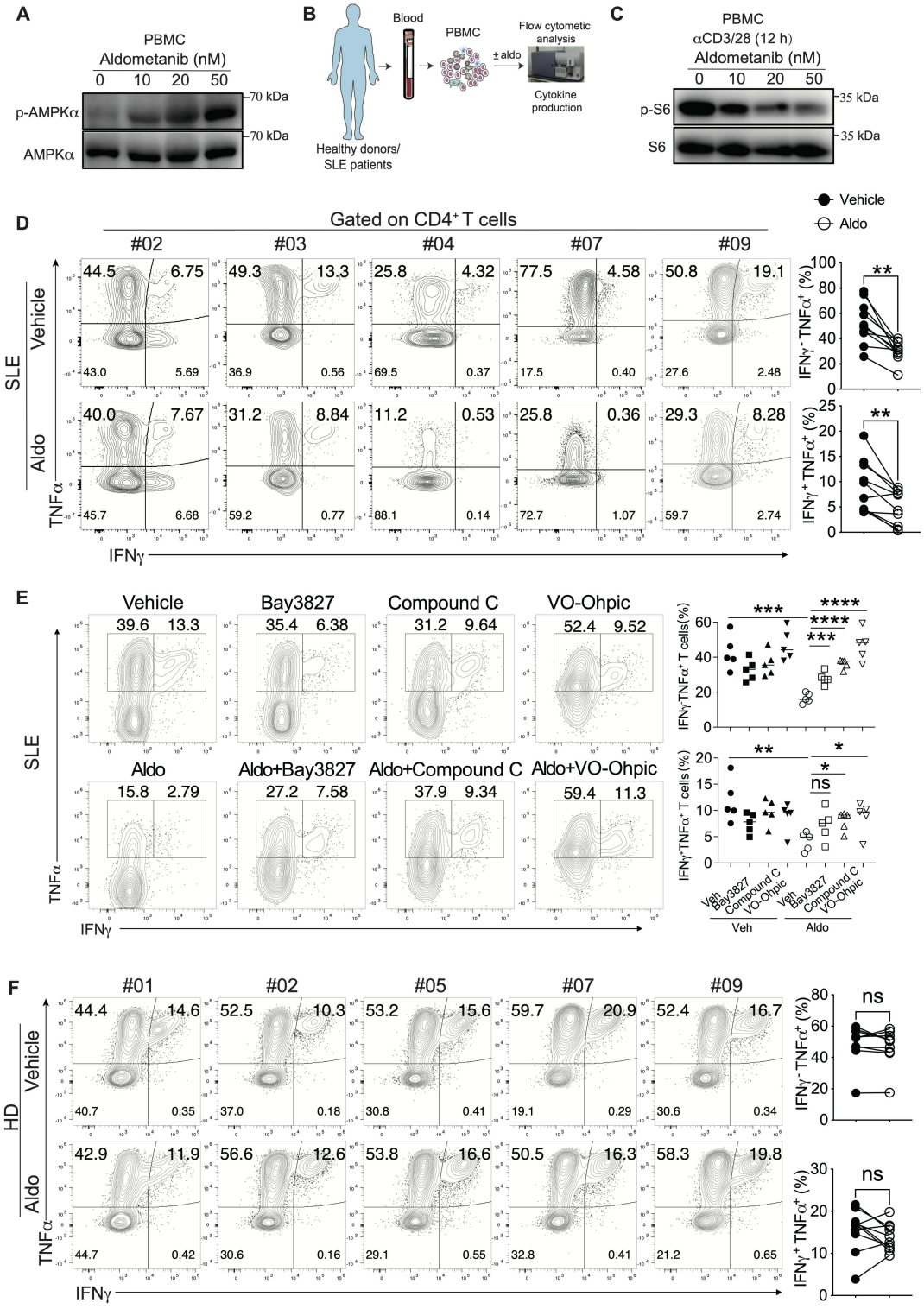

Fig. 8. Aldometanib suppresses proinflammatory cytokine secretion in T cells from PBMCs of SLE patients.

(A) Expression of phosphorylated AMPK in human T cells isolated from PBMCs, stimulated with anti-human CD3/CD28, and incubated with 0, 10, 20, or 50 nM aldometanib for 6 h. (B) Schematic workflow: peripheral blood was harvested from healthy donors and SLE patients for PBMC isolation. Isolated PBMCs were treated with aldometanib in vitro to detect alterations in T cell cytokine secretion. (C) Immunoblot detection of phosphorylated ribosomal S6 protein in

human T cells isolated from PBMCs, stimulated with anti-human CD3/CD28, and cultured with 0, 10, 20, or 50 nM aldometanib for 12 h. (D) Flow cytometric quantification of $CD4^+$ T cells producing IFN-γ and/or TNF-α in PBMCs isolated from SLE patients (n = 10 per group). (E) Effects of compound C (2μM) and Bay3827 (1 μM) and Vo-Ohpic (10 μM) on cytokine production by aldometanib-treated human $CD4^+$ T cells from SLE patients (n = 5). (F) Flow cytometric quantification of $CD4^+$ T cells producing IFN-γ and/or TNF-α in PBMCs isolated from healthy donors (n = 10 per group).